Quantum Monte Carlo Simulations of the Half-filled Hubbard Model

Anders F. J. Gabrielsson

June 2011

Abstract

A Quantum Monte Carlo method of calculating operator expectation values for the ground state of the nearest-neighbor Heisenberg model on large square lattices is presented, along with some comparisons of the results obtained from this method and alternative methods for 2D lattices. In the simulations the ground state is projected out from an arbitrary state and sampled in a valence bond basis spanning the spin singlet subspace. The projection method is then extended to be used on a simplified Hubbard model at half-filling, which is aptly called the T_0-less Hubbard model, for arbitrary relative strengths of the electron hopping and electron-electron repulsion energy parameters. Results for calculated ground state energies in 1D are presented. These calculations are performed using a spin-charge separated basis, in which the valence bonds are generalized to also carry charge.

Keywords:
Hubbard model, Heisenberg model, Projector quantum Monte Carlo, Ground state energy

Contents

Chapter 1

Introduction

In this Master thesis, a method of calculating ground state expectation values in two models related to the half-filled Hubbard model is studied.

A *projector quantum Monte Carlo method* as devised by Sandvik [7, 8] will be presented in the first part of the thesis, and then applied to the Heisenberg model on a 2D bipartite lattice. This method offers efficient ground state simulations for this model and is found to be easily implementable.

In the latter part, this projection method is extended to accommodate simulations of a related variant of the Hubbard model, the T_0*-less Hubbard model*, sharing some particular characteristics with the Heisenberg model which allow the construction of a similar projection method. As in the method developed by Sandvik, the operator of interest is evaluated by importance sampling by considering a Maarkov chain of projection strings. The main focus is defining a suitable basis for simulations of this model and generalize the approach of the projection method in Heisenberg model. Also, the algorithm for generating Metropolis steps in the sampling is given much attention, as the introduction of fermionic operators cause the projection to easily *break*, giving zero contribution to the evaluation of the sought expectation value.

The reader is expected to have basic understanding and experience with the notion of *second quantization*, which is commonly used in the context of quantum-many body theories. However, even skipping the technical parts where the operator manipulations leading to the central *rules of evaluation* used in the simulations are performed, the rather accessible graphical representation of the projection in the valence bond basis may help to give a basic idea of the physics and the results obtained.

The implementation is only described in abstract terms, and no knowledge of programming is required. Though, the material is probably more accessible for readers with some experience in computational physics and concepts such importance sampling.

Chapter 2

The Hubbard model

The Hubbard model is a lattice fermion model introduced to describe the interaction and correlation of electrons in crystalline solids. Using this model the *metal-insulator transition* of some materials, which are expected to behave as metals using the standard independent-electron band theory rather are insulators, and related magnetic phenomena can be described. It is also used to model basic aspects of the (not yet fully understood) physics in high-temperature cuprate superconductors [1, 2].

The picture to have in mind is a square lattice of ions, where the lower bands are filled and only one conducting band is available for the valence electrons to occupy. The Hubbard model is then based on two principal mechanisms in the interaction of these electrons; the tight-binding hopping of electrons between the lattice sites and the on-site Coulomb interaction of electrons positioned on the same site.

In a basis of *localized Wannier states*[1] the Hamiltonian of the Hubbard model can be written

$$\mathscr{H} = -t \sum_{\langle i,j \rangle} \sum_{\sigma=\uparrow,\downarrow} \left(c^\dagger_{i,\sigma} c_{j,\sigma} + c^\dagger_{j,\sigma} c_{i,\sigma} \right) + U \sum_i n_{i,\uparrow} n_{i,\downarrow} \,, \tag{2.1}$$

where the operators satisfy:

$$\begin{aligned} \{c_{i,\sigma}, c^\dagger_{j,\sigma'}\} &= \delta_{i,j}\delta_{\sigma,\sigma'} \,, \quad \{c_{i,\sigma}, c_{j,\sigma'}\} \;\; = 0 \\ n_{i,\sigma} &= c^\dagger_{i,\sigma} c_{i,\sigma} \,. \end{aligned} \tag{2.2}$$

The first part of the Hamiltonian is the same as in the tight-binding model, where the operator $c^\dagger_{i,\sigma}$ creates an electron with spin-orientation σ in the Wannier state of the band localized about lattice site i, and $c_{i,\sigma}$ is the corresponding

[1] See Appendix A for a formal definition of Wannier states in the context of the tight-binding model.

destruction operator. This part is called the band term or *kinetic term*, as it involves the motion (hopping) of the electrons in the crystal.

The second term in the Hubbard Hamiltonian is the on-site interaction. Two (opposite-spin) electrons occupying the same Wannier state will feel a strong Coulomb-repulsion, adding to the energy of such configuration.

In this version of the Hubbard model, one considers a crystal electron structure formed by only one Wannier state (atomic orbital) for each site, giving only one band in the kinetic term, i.e. the *single-band* Hubbard model. However, this band splits up into what is called two *Hubbard subbands*, separated by the energy on-site interaction U , as the energy spectrum of a single site becomes occupation number dependent by the on-site interaction term [1, pp 178-180]. The doubly-occupied states then make up the upper, high-energy subband, and the states not doubly occupied are included in the lower subband. Here, it is assumed that the energetic cost of introducing a doubly occupied state is large compared to the kinetic energy associated with the hopping processes, $t \ll U$. Low-energy states are then constructed by letting electrons occupy the lower subband before, after half-filling, starting to occupy the higher energy states in the upper subband. In this way the motion of the electrons in the low-energy sector is constrained, tending to avoid double occupation of a site, thus inducing correlation into the system.

Mott insulators and ceramic superconductors

With the surprising breakthrough of high-T_c cuprate superconductors in the second half of the 1980s, the interest of the Hubbard model was revived [2]. Unexplainable by conventional phonon-based Cooper pairing, it was found that the ceramic compound La_2CuO_4 becomes superconducting when doped by replacing a fraction of the lanthanum with barium.

In the resonating-valence-bond theory developed by Anderson, the interesting physics is essentially confined in layers of CuO_2 sandwiched between two layers of $[La, Ba]O$, in the characteristic layered quasi-2D structure of these cuprate superconductors. Pure La_2CuO_4 is in fact a *Mott insulator*, where the charge fluctuations associated with metallic conduction is suppressed by a strong on-site electron repulsion (giving a *large-U* Hubbard model, which is further discussed below), and in the context of the Hubbard model the relevant Wannier state on the lattice is a d-orbital of the ionized Cu^{2+}. The interaction between these Cu-ions then involves the intersite O^{2-} in a process called *super-exchange*. By this, the structure of the CuO_2 layer effectively becomes a square lattice for this electron correlation interaction (figure 2.1). When doped, each Ba introduced in the lattice removes one electron from the system, making the oxygen absorb one more electron from a Cu-ion to maintain the preferable O^{2-} configuration. The electron-holes associated with the created in this way become the metallic carriers [2], [3, p 38], [1, pp 217-220].

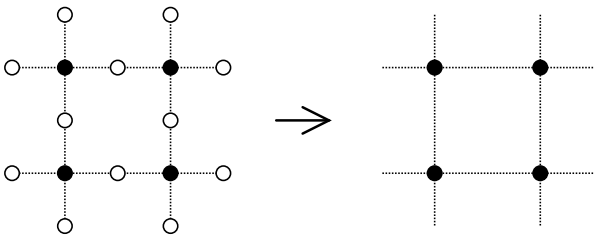

FIGURE 2.1: The valence interaction in the CuO_2 layer is effectively between electrons in a d-orbital of the ionized Cu (filled circles), reducing the topology of the system to a square lattice.

From this point of view, the studing the physics of (undoped) Mott insulating systems though the Hubbard model can be considered a testing ground for understanding high-T_c superconductivity.

2.1 The Heisenberg model

By applying a specific canonical transformation, one obtains an effective spin Hamiltonian valid in the limit $t/U \ll 1$. This is done by treating the kinetic term like a perturbation of the on-site interaction, mixing the approximate eigenstates corresponding to a fixed electron occupation number of each site. The kinetic term is split into a sum of three operators; T_+, T_0 and T_-, which includes the electron jumping processes resulting in an increase, conservation and decrease of the number of doubly occupied sites, respectively:

$$\mathscr{H} = t\,(T_- + T_0 + T_+) + U h_U\,, \tag{2.3}$$

with

$$\begin{aligned}
T_- &= -\sum_{\langle i,j\rangle}\sum_{\sigma}\Big((1-n_{i,-\sigma})c^\dagger_{i,\sigma}c_{j,\sigma}n_{j,-\sigma} + (1-n_{j,-\sigma})c^\dagger_{j,\sigma}c_{i,\sigma}n_{i,-\sigma}\Big)\\
T_0 &= -\sum_{\langle i,j\rangle}\sum_{\sigma}\Big((1-n_{i,-\sigma})c^\dagger_{i,\sigma}c_{j,\sigma}(1-n_{j,-\sigma}) + n_{i,-\sigma}c^\dagger_{i,\sigma}c_{j,\sigma}n_{j,-\sigma} + \text{H.C.}\Big)\\
T_+ &= -\sum_{\langle i,j\rangle}\sum_{\sigma}\Big(n_{i,-\sigma}c^\dagger_{i,\sigma}c_{j,\sigma}(1-n_{j,-\sigma}) + n_{j,-\sigma}c^\dagger_{j,\sigma}c_{i,\sigma}(1-n_{i,-\sigma})\Big)\,,
\end{aligned}$$

and

$$h_U = \sum_i n_{i,\uparrow}n_{i,\downarrow}\,.$$

Now, one wants to find a basis where the Hamiltonian is block diagonalized so that states of different number of doubly occupied sites are not mixed, making this a *good quantum number*. For large U, the ground state in this basis should be found in the low-energy subspace, consisting of states with no doubly occupied sites.

Applying the transformation

It is the terms T_- and T_+ that connect states in the two subbands, so the transformation is constructed to remove these. Writing the effective Hamiltonian from this transformation, denoting the generator S, as:

$$\mathscr{H}_{eff.} = \exp(iS)\mathscr{H}\exp(-iS) = \mathscr{H} + \frac{i[S,\mathscr{H}]}{1!} + \frac{i^2[S,[S,\mathscr{H}]]}{2!} + \dots , \quad (2.4)$$

it turns out that to prevent mixing to order t^2/U, a suitable choice of generator is [1, 4]:

$$S^{[2]} = -\frac{it}{U}(T_+ - T_-) + \frac{it^2}{U^2}\left[T_0, (T_+ + T_-)\right] .$$

Evaluating the commutators in the Campbell-Baker-Hausdorff expansion to second order with this generator, on finds:

$$i\left[S^{[2]}, \mathscr{H}\right] = -t(T_+ + T_-) + \frac{2t^2}{U}\left[T_+, T_-\right] + O(t^3/U^2) ,$$

and

$$\frac{i^2\left[S^{[2]}, [S^{[2]}, \mathscr{H}]\right]}{2!} = -\frac{t^2}{U}\left[T_+, T_-\right] + O(t^3/U^2) ,$$

so that the transformed second order Hamiltonian can be written:

$$\mathscr{H}^{[2]}_{eff.} = tT_0 + Uh_U + \frac{t^2}{U}[T_+, T_-] .$$

Although $\mathscr{H}^{[2]}_{eff.}$ does not mix states of the two subbands, the commutator gives the terms T_+T_- and T_-T_+, thus *virtually* changing the number of doubly occupied sites before restoring it again.

Considering the low-energy states at half-filling and with the on-site interaction energy U large enough so that each site is occupied by a single electron, as the cost of introducing doubly occupied site is comparably high. Then the terms tT_0 and Uh_U in the transformed Hamiltonian drops out as these are only non-zero for states with a non-zero number of holes and doubly occupied sites. Also, T_+T_- gives no contribution, as there are no doubly occupied states to remove, so the only interesting part is the term $-T_-T_+$. In the single-occupation subspace, this remaining term can be identified as [1, pp 207-208]

$$-T_-T_+ \doteq \sum_{\langle i,j\rangle} (4\boldsymbol{S}_i \cdot \boldsymbol{S}_j - 1) .$$

This expression describes the process of virtual hopping of opposite-spins neighbors as an effective spin-interaction, and from this the *anti-ferromagnetic*

Heisenberg model[2] is obtained:

$$\mathscr{H}_{HB} = J \sum_{\langle i,j \rangle} \left(\boldsymbol{S}_i \cdot \boldsymbol{S}_j - \frac{1}{4} \right) , \quad J = \frac{4t^2}{U} > 0 \, . \tag{2.5}$$

Note that although the ground state of this effective Hamiltonian, $|\Psi_0\rangle_{HB}$, has no doubly occupied sites (to second order, by construction), these are mixed back in when transforming back to the original basis of the Hubbard Hamiltonian:

$$\begin{aligned} |\Psi_0\rangle &= \exp(-iS) \, |\Psi_0\rangle_{HB} = (1 - \frac{t}{U}(T_+ - T_-) + \ldots) \, |\Psi_0\rangle_{HB} \\ &= |\Psi_0\rangle_{HB} - \frac{t}{U} T_+ \, |\Psi_0\rangle_{HB} + \ldots , \end{aligned} \tag{2.6}$$

where the states from $T_+ \, |\Psi_0\rangle_{HB}$ all contain a pair of double-occupied and non-occupied lattice sites.

2.2 The search for the ground state

Finding and characterizing the ground state is often taken as a starting point in the exploration of a model in physics. In quantum many-body systems like the Hubbard model and related models considered here, even this basic task can be anything but trivial as the dimensionality of the Hilbert space d_H, typically grows exponentially with the number of interacting particles. Adding to the burden, numerical routines for diagonalizing the Hamiltonian scale like $(d_h)^3$ [5, pp 594-596]. For the spin-half Heisenberg model of N spins, one finds $d_h = 2^N$ in a basis of S^z-eigenstates, and thus the scaling of the computational load is $\sim 2^{3N}$, which quickly becomes overwhelming as N is increased, regardless of the computational resources available.

Although exact numerical methods can be made much more efficient than suggested by this simplistic example[3], they are still often too slow for reliable extrapolation of physical quantities to the thermodynamical limit ($N \to \infty$). This leads to approximate methods such as Monte Carlo simulations, where accuracy of the result is traded for reduced running times and thus making larger systems accessible.

[2] Generally, the constant term is left out, but here it is included for convenience.

[3] The exact Heisenberg ground state energy has been computed for up to $N = 36$ (6×6 lattice), using the Lanczos diagonalization algorithm [6].

Chapter 3

Simulations of the Heisenberg Model

In this chapter, a computational technique for *projecting out* the ground state of the Heisenberg model and then calculating the corresponding energy, will be presented. The technique is based on the rather basic algorithm *power iteration* for obtaining an eigenvector for an operator, and the ground state is sampled by a Metropolis Monte Carlo scheme. A basis suitable for this projection-sampling called the *valence bond basis*, is also presented.

3.1 Power iteration

A simplistic approach for finding the eigenvector to a dominant eigenvalue for a matrix is through *power iteration*.

Consider a a diagonalizable $L \times L$-matrix M, with normalized eigenvectors $\boldsymbol{e}_i$ and the corresponding real positive eigenvalues λ_i, where λ_1 is the dominant eigenvalue. A random vector $\boldsymbol{v}_0$ can be expanded in this basis consisting of the eigenvectors[1]:

$$\boldsymbol{v}_0 = \sum_i c_i \boldsymbol{e}_i \,.$$

By operating on $\boldsymbol{v}_0$ by a large power of M, one obtains

$$M^k \boldsymbol{v}_0 = M^k \sum_i c_i \boldsymbol{e}_i = \sum_i c_i \lambda_i^k \boldsymbol{e}_i \,,$$

[1]This approach obviously breaks down if $\boldsymbol{v}_0 \perp \boldsymbol{e}_1$. However, when considering a random vector in $\mathbb{R}^d$ this occurs with probability 0.

which is approximately parallel to the eigenvector $\boldsymbol{e}_1$, as:

$$\left|\frac{M^k\boldsymbol{v}_0}{c_1\lambda_1^k}-\boldsymbol{e}_1\right| = \left|\sum_i \frac{c_i\lambda_i^k}{c_1\lambda_1^k}\boldsymbol{e}_i-\boldsymbol{e}_1\right| = \left|\sum_{i\geq 2} \frac{c_i\lambda_i^k}{c_1\lambda_1^k}\boldsymbol{e}_i\right| \leq \sum_{i\geq 2}\left|\frac{c_i}{c_1}\right|\left(\frac{\lambda_i}{\lambda_1}\right)^k ,$$

and $(\lambda_{i\geq 2}/\lambda_1)^k \to 0$, when $k\to\infty$. From this one can conclude that

$$\boldsymbol{v}_k \equiv \frac{M^k\boldsymbol{v}_0}{|M^k\boldsymbol{v}_0|} \to \boldsymbol{e}_1 , \quad k\to\infty .$$

This approach is now carried over to the problem of finding, or *projecting out*, the ground state of a Hamiltonian where exact diagonalization is not practically feasible. First one needs to make sure that the lowest energy state correspond to the dominant eigenvalue. For systems with a finite upper bound of the energy this is easily done by shifting the spectrum with a constant C, so that the highest energy correspond to zero. The ground state energy must then be negative, so one may also reverse the spectrum to retain a positive sign in the power iteration. Now the operator that projects out the ground state can be written:

$$\pi \equiv \frac{1}{\Omega^k}\left(-(\mathscr{H}-C)\right)^k , \quad k\to\infty , \tag{3.1}$$

where a normalization factor $\Omega = -(E_0 - C)$ (containing the actual value of ground state energy E_0), has been added.

Starting with some random initial state expanded in a basis of energy eigenstates

$$|\phi\rangle = \sum_n c_n |E_n\rangle ,$$

the ground state is *projected out* by the operator defined in (3.1):

$$\pi|\phi\rangle = \frac{1}{\Omega^k}\left(C-\mathscr{H}\right)^k \sum_n c_n|E_n\rangle \;\to\; c_0|E_0\rangle , \quad k\to\infty .$$

3.2 Projector quantum Monte Carlo

As the ground state of the spin-half Heisenberg model for on a *bipartite lattice* of an even number of sites N, is a singlet ($S_{tot}=0$) [9], it can be can be expanded in a *valence bond basis* [10]:

$$|GS\rangle = \sum_V f_V |V\rangle , \quad f_V \geq 0 ,$$

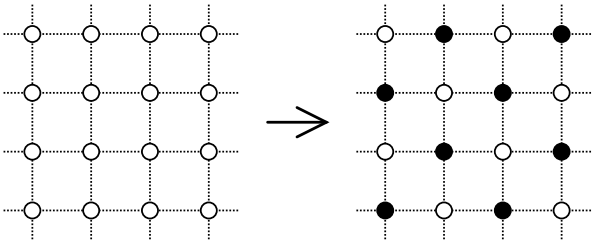

FIGURE 3.1: The sites of the square lattice is divided into two sublattices with the sites A and B (filled). Here, periodic lattices are considered, giving the topology of a torus.

where the basis states correspond to a specific pairing of the N spins (for lattice size N) into $N/2$ singlets:

$$|V\rangle = \big|(a_1, b_1), (a_2, b_2) \dots (a_{N/2}, b_{N/2})\big\rangle \ , \quad (a, b) \equiv \frac{1}{\sqrt{2}}\big(|\uparrow_a\downarrow_b\rangle - |\downarrow_a\uparrow_b\rangle \big) \, .$$

Further, the basis can be restricted to only include valence bond state consisting of singlets with the sites labeled a and b belonging to the two sublattices A and B, respectively (figure 3.1).

3.2.1 The projection operator

The Heisenberg Hamiltonian (2.5) is now written in terms of *singlet projection operators*, Q_{ij}:

$$\mathscr{H}_{HB} = -J \sum_{\langle i,j \rangle} Q_{ij} \, , \quad Q_{ij} \equiv \frac{1}{4} - \boldsymbol{S}_i \cdot \boldsymbol{S}_j \, ,$$

where the action of these operators on a valence bond state are[2]:

$$\begin{aligned} Q_{ij} \, |\dots (i, j) \dots\rangle &= |\dots (i, j) \dots\rangle \\ Q_{ij} \, |\dots (i, l) \dots (k, j) \dots\rangle &= \frac{1}{2} \, |\dots (i, j) \dots (k, l) \dots\rangle \ . \end{aligned} \tag{3.2}$$

So the singlet projection operator Q_{ij} forms a singlet of the spins at site $i \in A$ and $j \in B$, and any spins that previously formed singlets with these, now form another singlet, as in shown in figure 3.2.

From the form of the Hamiltonian (2.5) it is clear that the highest eigenvalue is 0, corresponding to completely aligned spins. The energy spectrum is then already negative semi-definite, and one may omit the shifting constant C i the ground state projection operator (3.1), so it is written:

$$\pi = \frac{1}{\Omega^k} \left(J \sum_{\langle i,j \rangle} Q_{ij} \right)^k \, , \quad k \to \infty \, , \Omega = -E_0 \, .$$

[2]See Appendix C for a formal treatment of the valence bond basis and the evaluation rules for the singlet projection operator.

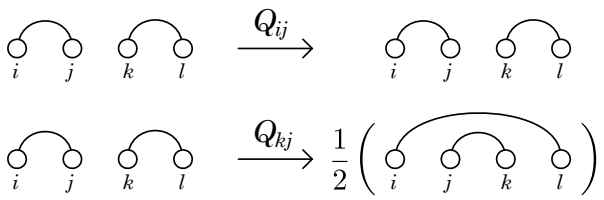

FIGURE 3.2: The action of the singlet projection operator onto valence bond states with $i, k \in A$ and $j, l \in B$. The valence bonds are represented by lines connecting the sites of which the spins form singlets. In the second example the state is modified by *rewiring* the bonds, and also a factor $1/2$ is introduced.

For finite k, one may expand the k-factor product of sums of projection operators to a sum of products[3]:

$$\pi^{(k)} = \left(\frac{J}{\Omega}\right)^k \sum_r \left(\coprod_p Q^{(r)}_{i_p j_p} \right) = \left(\frac{J}{\Omega}\right)^k \sum_r P^{(k)}_r \,, \tag{3.3}$$

where $P^{(k)}_r$ is a product, or an *operator string*, of k singlet projection operators:

$$P^{(k)}_r \equiv \coprod_{p=1}^{k} Q^{(r)}_{i_p j_p} = Q_{i_k j_k} \dots Q_{i_2 j_2} Q_{i_1 j_1} \,,$$

and the sum $\sum_r P^{(k)}_r$ contains all $(zN/2)^k$ possible k-length strings of singlet projection operators, where z is the coordination number, i.e. the number of nearest-neighbors for each site in the lattice.

Applying a projection string $P^{(k)}_r$, onto an initial valence bond state $|V_0\rangle$, yields a modified valence bond state as in figure 3.3. The propagated state has amplitude w_r depending on m; the number of times the operators in the string causes a reconfiguration of the singlets in the propagating valence bond state:

$$P^{(k)}_r |V_0\rangle = w_r |V_r\rangle \,, \quad w_r = 1/2^m \,. \tag{3.4}$$

As the ground state and its properties are not know before actually performing the calculation, the value of Ω in (3.3) and the expansion coefficient for the initial state in the eigenstate basis are unknown, but an expression for the ground state of the Heisenberg model expanded in the valence bond basis

[3]The silly notation used here regarding the product sequence symbol suggests that the order of the factors in the sequence is reversed. This is so as one would like to call the rightmost operator the *first* etc. as it is in this order they will be evaluated when acting upon a ket-state.

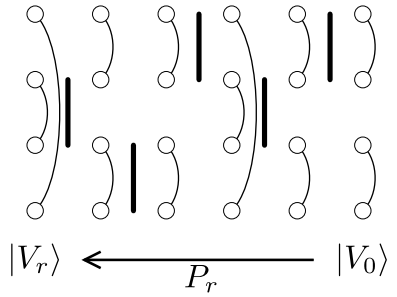

FIGURE 3.3: The initial state $|V_0\rangle$ is projected by the string P_r of length $k = 5$, giving the projected state $|V_r\rangle$. The singlet projection operators Q_{ij}, in the projection string are represented by bold lines indicating onto which lattice site pair they are operating. Here, the amplitude is not shown, but in this example $w_r = (1/2)^3 = 1/8$, as three operators reconfigure the singlet pairings during the propagation.

is obtained, up to a normalization factor by use of the truncated projection operator and any initial valence bond state:

$$|GS\rangle \sim \sum_r P_r^{(k)} |V_0\rangle = \sum_r w_r |V_r\rangle \ , \quad k \to \infty \, . \tag{3.5}$$

3.2.2 Calculating the GSE by importance sampling

As the Hamiltonian can be written as a sum of singlet projection operators, the action of it on a valence bond state gives a linear combination of modified valence bond states:

$$\mathscr{H} |V_r\rangle = J \sum_{\langle i,j \rangle} -Q_{ij} |V_r\rangle = J \sum_b h_b^{(r)} |V_r^{(b)}\rangle \ , \quad h_b = -1 \text{ or } -1/2 \, , \tag{3.6}$$

where the values of $h_b^{(r)}$ are given by the expression (3.2) for the corresponding singlet projector $-Q_{ij}$.

Now one can write an expression for the ground state energy by using the expression (3.5) for the projected ground state, in which the unknown normalization factor cancels:

$$E_0 = E_0 \frac{\langle \psi | GS \rangle}{\langle \psi | GS \rangle} = \frac{\langle \psi | \mathscr{H} | GS \rangle}{\langle \psi | GS \rangle} = \frac{\langle \psi | \mathscr{H} \left(\sum_r P_r^{(k)} |V_0\rangle \right)}{\langle \psi | \left(\sum_r P_r^{(k)} |V_0\rangle \right)} \, , \quad k \to \infty$$

and letting the projection strings act on the initial state, one finds:

$$E_0 = \frac{\sum_r w_r \langle \psi | \mathscr{H} | V_r \rangle}{\sum_r w_r \langle \psi | V_r \rangle} = \frac{\sum_r w_r \left(J \sum_b h_b^{(r)} \langle \psi | V_r^{(b)} \rangle \right)}{\sum_r w_r \langle \psi | V_r \rangle} \, .$$

The state $|\psi\rangle$ used here is arbitrary as long as it has a non-zero overlap with the ground state, but it is convenient to use the classical anti-ferromagnetic (staggered) Néel state:

$$|\Psi_N\rangle = |\sigma_1, \sigma_2, \ldots, \sigma_N\rangle \ , \quad \sigma_i = \begin{cases} \uparrow, & i \in A \\ \downarrow, & i \in B \end{cases}$$

for which every valence bond state has an equal overlap: $\langle \Psi_N | V \rangle = \left(1/\sqrt{2}\right)^{N/2}$. The expression for the ground state energy then simplifies to:

$$E_0 = \frac{\sum_r w_r \left(J \sum_b h_b^{(r)} \right)}{\sum_r w_r} \, . \tag{3.7}$$

This expression is not variational in the sense that for finite k the physical interpretation is not well defined. Nevertheless, in the limit of large k corresponding to infinitely long projector strings, it becomes an exact expression for the ground state energy.

Noting that the form of the expression (3.7) resembles an expectation value of some stochastic variable $e_r = \sum_b h_b^{(r)}$ using a probability distribution, or weight, w_r, one can evaluate the expression by employing a Monte Carlo algorithm to sample over the possible projector strings, giving the name *projector Monte Carlo* (PMC). This stochastic interpretation is valid since all weights are positive definite from (3.4), so the ground state energy (in units of J) is obtained by evaluating:

$$E_0/J = \sum_r \frac{w_r}{Z} e_r \, , \quad Z = \sum_r w_r \, .$$

Sampling of the operator strings is then done by utilizing the *Metropolis algorithm*[4] to generate a random walk through the possible configurations of the singlet operators in a operator string of length k, with distribution according to the weight w_r/Z.

Outline of sampling process

Following the standard Metropolis algorithm, each step in the importance sampling is divided into two parts. Starting in some configuration, a *trial* configuration is generated which is then *accepted* with some probability or else *rejected*. After this, the estimator corresponding to the last accepted configuration is evaluated and sampled. The mean value of these samples then constitute the approximate value of the quantity in question.

After constructing some suitable initial valence bond state $|V_0\rangle$, an initial (finite length) string of singlet operators P, is created. The weight w of this string is

[4] See Appendix D for a basic introduction to Monte Carlo simulations and the concepts used in the following.

obtained by *propagating* the initial state, evaluating the action of each operator in order according to rules in (3.2). Now a trial string, P' is constructed by translating[5] a number of singlet projection operators in P:

$$P = Q_{i_k j_k} \dots \underline{Q_{i_r j_r}} \dots Q_{i_1 j_1} \quad \xrightarrow{update} \quad P' = Q_{i_k j_k} \dots \underline{Q_{i'_r j'_r}} \dots Q_{i_1 j_1} \,.$$

Then $|V_0\rangle$ is propagated with this modified string, and the corresponding weight w' is obtained. This reconfiguration of the operators is accepted, letting $P \to P'$ with probability $p_{acc.} = \min(w'/w, 1)$, else the trial string is discarded. For each step the energy estimator is evaluated for the propagated state $|V_P\rangle = P\,|V_0\rangle$ by (3.6) and sampled.

In this updating scheme the average acceptance rate can easily be adjusted by changing the number of operators translated in generating the trial strings. Note that the initial valence bond state $|V_0\rangle$, which the generated strings operate upon, is kept fixed during the sampling, and only the projection strings themselves are modified.

Detailed balance and ergodicity

With this construction, the composite transition probability in a specific update is given by

$$p(P \to P') = p_{sugg.}(P \to P') p_{acc.}(P \to P') \,,$$

with $p_{sugg.}(P \to P')$ being the probability of obtaining the string P' from P when randomly translating the specified number of operators. If the singlet operators chosen to be translated in the construction of the trial string are chosen uniformly, and also the pair of lattice sites which the operator is translated to operate onto, then this *suggestion* or *candidate-generating function* is clearly symmetric, meaning:

$$p_{sugg.}(P \to P') = p_{sugg.}(P' \to P) \,.$$

Using the acceptance probability as above the transition probability in this updating scheme satisfies the condition of *detailed balance* [11, pp 196-199]:

$$\frac{p(P \to P')}{p(P' \to P)} = \frac{p_{acc.}(P \to P')}{p_{acc.}(P' \to P)} = \frac{\min(w'/w, 1)}{\min(w/w', 1)} = \frac{w'}{w} \,.$$

Also, the random walk generated by this updating scheme is clearly *non-cyclic* and *irreducible*, as the probability of trivial updates (operators are translated to their original position) is non-zero for any projection string and for obtaining any given string there exists an updating sequence corresponding to simply transversing any other string, updating the operators to the specified configuration. From this one concludes that the generated Markov chain is *ergodic*, and the sampling scheme will sample operator strings with probability proportional to their weights, as intended.

[5] *Translate* here means change onto which lattice sites the operator is acting.

Details of the implementation

For all systems, first a set of *convergence runs* are setup where the projector string length, k, used is increased for each run until the value for the computed quantity converges within the statistical error of the importance sampling. Then it can be argued that k is large enough for the sampled quantity to be a good approximation of the ground state expectation value.

To increase the efficiency of the importance sampling by reducing the projection length used, a *pre-projection* is carried out for each run. This is done similarly to the standard *relaxation*, where the samples from the initial period in the run are discarded, removing any dependence of the specific choice of initial configuration for the simulation. When performing the pre-projection, the projected state $|V_r\rangle = P_r |V_0\rangle$ found after the initial relaxation period replaces the original initial state in the subsequent projections: $|V_0'\rangle = |V_r\rangle$. After the projection string is then re-relaxed, sampling may begin.

3.3 Variational expression for arbitrary operators

The form of the expression for the ground state energy (3.7) was based on the defining property of the Hamiltonian being diagonal in a basis of energy eigenstates, and in a similar form any operator diagonal in this basis can be expressed. An expression for the expectance value of an arbitrary operator, not necessarily simultaneously diagonalizable with the Hamiltonian, can be obtained in a *two-sided projection*:

$$\langle \mathscr{A} \rangle_{GS} = \frac{\sum_{l,r} \langle V_0' | P_l^\dagger \mathscr{A} P_r | V_0 \rangle}{\sum_{l,r} \langle V_0' | P_l^\dagger P_r | V_0 \rangle} = \frac{\sum_{l,r} w_l w_r \langle V_l | \mathscr{A} | V_r \rangle}{\sum_{l,r} w_l w_r \langle V_l | V_r \rangle} \,. \tag{3.8}$$

The overlap of the valence bond states can be evaluated by finding the *bond loops* formed by superimposing the singlet pairing of the two states onto the lattice [10]. The overlap is then found to be

$$\langle V_l | V_r \rangle = 2^{N_l - N_b} \,,$$

where N_l is the number of closed loops formed by the overlapping valance bond states and $N_b = N/2$ is the number of bonds in the state. See figure 3.4 for an illustrated example.

Then one may use $W_{l,r} = w_l w_r \langle V_l | V_r \rangle$ as a weight in the sampling as all factors are positive-definite, and one obtains the expression:

$$\langle \mathscr{A} \rangle_{GS} = \frac{\sum_{l,r} W_{l,r} \, a_{l,r}}{\sum_{l,r} W_{l,r}} \,, \quad a_{l,r} = \frac{\langle V_l | \mathscr{A} | V_r \rangle}{\langle V_l | V_r \rangle} \,.$$

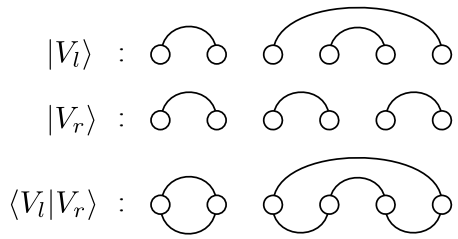

FIGURE 3.4: The overlap of two valence bond states is computed by counting the bond-loops formed when overlaying the states. In this example $\langle V_l|V_r\rangle = 2^{2-3} = 1/2$.

TABLE 3.1: Calculated E_0 by PMC compared to [6].

L	$N = L \times L$	E_0^{PMC}/JN	E_0^{ref}/JN	k	n_{MCS}
4	16	$-1.201(41)$	-1.20178	64	$4.8 \cdot 10^5$
6	36	$-1.178(22)$	-1.17887	144	$1.9 \cdot 10^6$
8	64	$-1.173(17)$	-1.17349	256	$4.3 \cdot 10^6$
12	144	$-1.1707(6)$	-1.17069	576	$7.7 \cdot 10^6$
16	256	$-1.1699(6)$	-1.16998	1024	$3.1 \cdot 10^7$

Spin correlation function

A particularly interesting operator that can easily be evaluated in the VB basis is the spin correlation function, $\boldsymbol{S}_i \cdot \boldsymbol{S}_j$. The estimator for this operator can also be evaluated by using bond loops, and it is found to be [10]:

$$\frac{\langle V_l|\boldsymbol{S}_i \cdot \boldsymbol{S}_j|V_r\rangle}{\langle V_l|V_r\rangle} = \begin{cases} +3/4\,, & i,j \text{ in same loop and on same sublattice} \\ -3/4\,, & i,j \text{ in same loop but on opposing sublattices} \\ 0\,, & i,j \text{ in different loops.} \end{cases}$$

3.4 Results for the Heisenberg model

Simulations where performed on square lattices, with sizes ranging from 4×4 ($N = 16$) to 16×16 ($N = 256$), calculating the Heisenberg ground state energies of these systems. In table 3.1 and figure 3.5 values of per-site E_0 obtained by the PMC method is presented, expressed in units of the interaction strength parameter J. The calculated energies are compared to accurate values obtained by the *stochastic series expansion* Monte Carlo method [6], where the values are shifted by $-JN/2$ to account for the slightly different form of the Heisenberg Hamiltonian used.

The statistical error is estimated by performing a number of independent runs (independent *walkers*) for each set of parameters. In these simulations ten walkers are used, and the accuracy is given as the standard deviation of the results from the walkers. This method of error estimation can be considered

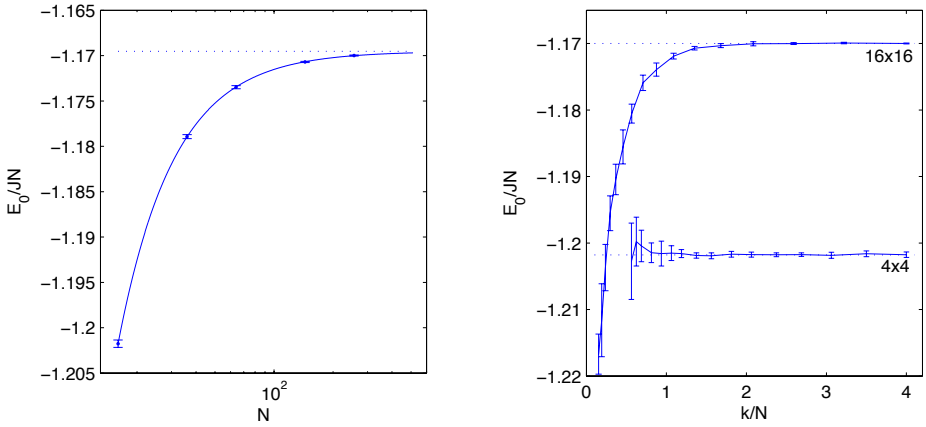

(a) Ground state energy, $E_0(N)$.

(b) Convergence of $E_0(N)$ in k.

FIGURE 3.5: Per-site ground state energies of 2D Heisenberg model by PMQ. To the left results from simulations are shown with a fitted power function and the large-N limit. In these simulations projection string length $k = 4N$ is used and $3 \cdot 10^4\, k$ samples divided over 10 walkers. Data from two convergence runs are also shown, where k is varied (right).

wasteful and *inaccurate*, as each walker must perform the costly relaxing procedure independently and when a only small number of walkers is used, the error estimation itself may exhibit significant statistical fluctuations [12]. Nevertheless, this method is found to be easily implemented and fairly robust for automated error estimations, as when performing the large number of runs necessary for the k-convergence test.

Scaling of simulation time

If a suitable length of the projection string follows $k \sim N^{\gamma_k}$, and the number of samples generated in each run is set to $n_{MCS} \sim k^{\gamma_n}$ to obtain some given statistical accuracy, then the simulation time scales like $k \cdot n_{MCS} \sim N^{\gamma_k(1+\gamma_n)}$. Here, projector string length $k = 4N$ is chosen and the number of samples generated in each run is $n_{MCS} = 3 \cdot 10^4\, k$ with $m = 4$ operators updated in each trial string, thus $\gamma_k, \gamma_n = 1$ is set and simulation time scales $\sim N^2$.

As seen, the sampling accuracy is increasing with system size with this scaling of parameters, suggesting $\gamma_n < 1$ could be used, reducing the scaling of simulation time. The running time for the largest lattice considered here (16×16) is roughly half an hour on a standard (by 2010) single-CPU personal computer.

Extrapolation of E_0

Given the high accuracy of the calculated ground state energies it is tempting to try fitting the obtained values to some analytical expression for the ground state energy for arbitrary lattice sizes, $E_0^*(N)$, to make a rudimentary approximation of E_0 in the thermodynamical limit. To this end a fit of the calculated energies is made for a power function:

$$E_0^*(N)/JN = a\,N^b + c\,,$$

and from the simulation data in table 3.1, the parameters are obtained:

$$a^* = -2.1674\,, \quad b^* = -1.5179\,, \quad c^* = -1.1695\,.$$

From this one has an approximation of $E_0(N \to \infty)$ readily available:

$$\lim_{N\to\infty} E_0^*(N)/JN = -1.1695\,.$$

This is a over-estimation of the ground state magnitude, as $E_0/JN = -1.16945$ for a 64×64-system as computed in [7].

Chapter 4

Simulations of the T_0-less Hubbard model

In the previous chapter the Heisenberg model was obtained from the half-filled Hubbard model in a special treatment for $t/U \to 0$, and using a Projector Monte Carlo technique the ground state was sampled in the valence bond basis. Here, a different transformation will be applied to a slightly modified Hubbard model, lacking the T_0 term in the Hamiltonian, and adapt the sampling scheme to run simulations of this electronic system for finite values of t/U.

4.1 Spin-charge separation

The *quasiparticle operators* $\tilde{c}_r$ and q_r^i are defined using the ordinary electron (Wannier state) creation operators $c_r^\dagger$ [13]:

$$\begin{aligned}
\tilde{c}_r &= c_{\uparrow,r}^\dagger(1-n_{\downarrow,r}) + (-1)^r c_{\uparrow,r} n_{\downarrow,r}\,, \\
q_r^+ &= (c_{\uparrow,r}^\dagger - (-1)^r c_{\uparrow,r}) c_{\downarrow,r}\,, \\
q_r^- &= (q_r^+)^\dagger\,, \\
q_r^z &= \frac{1}{2} - n_{\downarrow,r}\,,
\end{aligned}$$

It can be verified that the operators defined by this satisfies:

$$\begin{aligned}
&\{\tilde{c}_r, \tilde{c}_{r'}^\dagger\} = \delta_{rr'}\,, \qquad \{\tilde{c}_r^\dagger, \tilde{c}_{r'}^\dagger\} = 0\,, \\
&[\tilde{c}_r^\dagger, q_{r'}] = 0\,, \qquad\quad [q_r^i, q_{r'}^j] = i\delta \sum_k \epsilon_{ijk} q_r^k\,,
\end{aligned}$$

with

$$q_r^x = \frac{1}{2}(q_r^+ + q_r^-)\,, \quad q_r^y = \frac{1}{2i}(q_r^+ - q_r^-)\,.$$

Thus, $\tilde{c}_r^\dagger$ is a fermionic charge-like quasiparticle, and q_r^i obey the $SU(2)$ algebra associated with spin-half bosons, and by this transformation the spin and charge in the electron system is separated.

Using these quasi-particle operators, the half-filled Hubbard Hamiltonian

$$\mathscr{H} = t(T_- + T_0 + T_+) + Uh_U \,,$$

is rewritten in the spin-charge separated form, where the electron jumping part becomes:

$$\begin{aligned}
T_- &= 2\sum_{\langle r,r'\rangle} (-1)^r \left(\frac{1}{4} - \boldsymbol{q}_r \cdot \boldsymbol{q}_{r'}\right) \tilde{c}_{r'}\tilde{c}_r \,, \\
T_0 &= 2\sum_{\langle r,r'\rangle} \left(\frac{1}{4} + \boldsymbol{q}_r \cdot \boldsymbol{q}_{r'}\right) (\tilde{c}_r^\dagger \tilde{c}_{r'} + \tilde{c}_{r'}^\dagger \tilde{c}_r) \,, \\
T_+ &= 2\sum_{\langle r,r'\rangle} (-1)^r \left(\frac{1}{4} - \boldsymbol{q}_r \cdot \boldsymbol{q}_{r'}\right) \tilde{c}_r^\dagger \tilde{c}_{r'}^\dagger \,,
\end{aligned}$$

and the on-site interaction term:

$$h_U = \frac{1}{2}\sum_r \tilde{c}_r^\dagger \tilde{c}_r \,.$$

Here $(-1)^r = -1$ for $r \in A$ and $(-1)^{r'} = 1$ for $r' \in B$ is defined, and in the following it is assumed that the indices of the operators refer to A and B sites as written above.

One can now observe that the transformed T_- and T_+ operators are singlet projection operators in quasi-spin space, with quasi-charge operators attached. As presented earlier, it is the T_- and T_+ operators that introduces fluctuations of the number of doubly occupied sites (and holes) in the lattice, and it can be seen from the definition of the quasi operators that the creation of a pair of quasi charges in the transformed system correspond to the creation of a doubly occupied site and hole pair in the (original) Hubbard model.

4.1.1 A T_0-less Hubbard model

To retain the significative mechanism of *charge density fluctuation* of the Hubbard model, but still allow for the quasi-spin part to be handled in terms of singlet projection in the valence bond basis as in PMC for the Heisenberg model, the incompatible T_0 term is valorously left out and one obtains the T_0*-less Hubbard model*, which will be the subject of the following work:

$$\tilde{\mathscr{H}} = t(T_- + T_+) + Uh_U \,.$$

As with the complete Hubbard model, the Heisenberg model is obtained in the limit $t/U \to 0$ by letting $T_0 \to 0$ when performing the large-U transformation (2.4), and so the models can be considered to be equivalent in this limit.

4.2 PMC for the T_0-less Hubbard model

The aim now is to construct a projector Monte Carlo method of computing ground state properties of the model.

4.2.1 The charge decorated valence bond basis

For finite t/U the simulation must also allow for quasi charge fluctuations, corresponding to states with a non-zero number of double occupied sites and holes, so the basis used has to be adapted for this. To this end, one may consider a *quasi charge-decorated quasi spin valence bond basis*, where the quasi charges are added to quasi spin-singlet states.

The basis used is restricted to AB-singlet pairs, as for the Heisenberg model, and the restriction that the charge configurations of the basis states are such that both sites in each singlet carries equal quasi charge is also imposed. In this sense one can talk of *charged* and *uncharged singlets*, referring to sites paired in a valence bond and their (equal) quasi charge state. As before, the singlet states are expressed in terms of valence bond operators, but now these are extended to also form charged states. The operator creating uncharged singlets is defined analogously to the ordinary singlet creation operator:

$$\tilde{\chi}^{0\dagger}_{ij}\,|vac\rangle = \frac{1}{\sqrt{2}}\Big(\,|\uparrow_i\downarrow_j\rangle - |\downarrow_i\uparrow_j\rangle\,\Big)\otimes|\circ_i\circ_j\rangle\ ,$$

and the charged singlets are created by the charge decorated operator:

$$\tilde{c}^{\dagger}_i\tilde{c}^{\dagger}_j\tilde{\chi}^{0\dagger}_{ij}\,|vac\rangle = \frac{1}{\sqrt{2}}\Big(\,|\uparrow_i\downarrow_j\rangle - |\downarrow_i\uparrow_j\rangle\,\Big)\otimes|\bullet_i\bullet_j\rangle\ ,$$

where the arrows denote quasi spin states, and $\bullet$ (or $\circ$) denote sites carrying quasi charges (or no charges) respectively, with $i \in A$ and $j \in B$.

As quasi and ordinary spin coincide in the quasi charge or double occupancy free sector, one can conclude that the ground state of the corresponding quasi spin Heisenberg model is found in the quasi spin singlet sector, spanned by a (quasi charge-less) quasi spin valence bond basis, analogous to the similar treatment in the original Hubbard model [13]. From this it is clear that the ground state for the T_0-less model in the limit $t/U \to 0$ can be expanded in this charge decorated valence bond basis. The restriction to only consider equal charged sites in the singlets can be argued to be valid, since T_+ and T_- preserve *sub-lattice charge balance*[1], and the basis states in the subspace considered can be formed by repeated application of these operators onto the uncharged singlet ground state.

[1] What is called *the sub-lattice charge balance* is given by $\sum_{i\in A}\tilde{n}_i - \sum_{j\in B}\tilde{n}_j$.

$T_\pm$ acting on charge decorated valence bond states

Including the quasi charges, the rules for evaluating the action of the terms in the T_0-less Hamiltonian onto the charge decorated valence bond states become slightly more complicated than the corresponding rules for the ordinary spin projection operators found in the Heisenberg Hamiltonian[2]. Writing some charge decorated valence bond state $|\tilde{V}\rangle$ of N-sites, where M of the $N/2$ singlets are charged, and the other M' singlets are uncharged:

$$|\tilde{V}\rangle = \prod_{s=1}^{M} \left(\tilde{c}^\dagger_{a_s} \tilde{c}^\dagger_{b_s} \tilde{\chi}^{0\dagger}_{a_s b_s} \right) \prod_{s=1}^{M'} \left(\tilde{\chi}^{0\dagger}_{a'_s b'_s} \right) |vac\rangle \ , \tag{4.1}$$

with $M + M' = N/2$ and $\{a_s\} \cap \{a'_s\} = \{b_s\} \cap \{b'_s\} = \emptyset$, so that each site of the lattice is included in exactly one singlet-pair factor. Note that the ordering of the charge decorated valence bond operators in the first product is arbitrary, as the charge operators always are written in the AB pairs corresponding to the singlet operator, and $\left[\tilde{c}^\dagger_i \tilde{c}^\dagger_j \, , \tilde{c}^\dagger_k \tilde{c}^\dagger_l \right] = 0$, when the indices are unique.

Obviously, all states formed in this way have a well defined charge state, and are eigenstates of the on-site interaction term:

$$h^{(U)}_r \, |\tilde{V}\rangle = \frac{1}{2} \tilde{n}_r \, |\tilde{V}\rangle \ .$$

The kinetic terms are expressed by writing the singlet projection using the charge decorated valence bond operators[3]:

$$\left(\frac{1}{4} - \boldsymbol{q}_r \cdot \boldsymbol{q}_{r'} \right) = \tilde{Q}_{rr'} = \tilde{\chi}^{0\dagger}_{rr'} \tilde{\chi}^{0}_{rr'} \, ,$$

and so:

$$T^{(+)}_{rr'} = 2 \, \tilde{c}^\dagger_r \tilde{c}^\dagger_{r'} \tilde{\chi}^{0\dagger}_{rr'} \tilde{\chi}^{0}_{rr'} \, , \quad T^{(-)}_{rr'} = 2 \, \tilde{c}_{r'} \tilde{c}_r \tilde{\chi}^{0\dagger}_{rr'} \tilde{\chi}^{0}_{rr'} \, .$$

One may observe that these charge decorated singlet projection operators annihilate any state where the sites onto which it operates, (here labeled r and r') are not equally charged, as the quasi charge operators are fermionic.

In the case of matching charge states, first consider the operation onto two uncharged neighboring sites when only the $T^{(+)}_{rr'}$ terms are active. Dropping the 2 in $T^{(+)}_{rr'}$, consider the operator $\tilde{c}^\dagger_i \tilde{c}^\dagger_j \tilde{\chi}^{0\dagger}_{ij} \tilde{\chi}^{0}_{ij}$, where i and j matches two indices in $\{a'_s\}$ and $\{b'_s\}$ in the product of uncharged valence bond operators as written in (4.1). The result is a modified charge decorated valence bond state, where the quasi particles on sites i and j form a charged singlet:

$$\tilde{c}^\dagger_i \tilde{c}^\dagger_j \tilde{\chi}^{0\dagger}_{ij} \tilde{\chi}^{0}_{ij} \, |\tilde{V}\rangle = \tilde{c}^\dagger_i \tilde{c}^\dagger_j \tilde{\chi}^{0\dagger}_{ij} \prod_{s=1}^{M} \left(\tilde{c}^\dagger_{a_s} \tilde{c}^\dagger_{b_s} \tilde{\chi}^{0\dagger}_{a_s b_s} \right) \left[\tilde{\chi}^{0}_{ij} \, ; \prod_{s=1}^{M'} \tilde{\chi}^{0\dagger}_{a'_s b'_s} \right] |vac\rangle \ .$$

[2]The impatient reader may refer to figure 4.1 where the results from these calculations are encapsulated in a graphical representation.

[3]The valence bond operators are defined in Appendix C.

The spin part of the operation follow the same rules as in the treatment of the ordinary singlet projection operators. For $(i,j) \in \{(a'_s, b'_s)\}$, one evaluate the commutator as[4]:

$$\left[\tilde{\chi}^0_{ij}\,; \prod_{s=1}^{M'} \tilde{\chi}^{0\dagger}_{a'_s b'_s}\right] |vac\rangle = \left[\tilde{\chi}^0_{ij}\,, \tilde{\chi}^{0\dagger}_{ij}\right] \prod_{s=1}^{M'-1} \tilde{\chi}^{0\dagger}_{a'_s b'_s} |vac\rangle = \prod_{s=1}^{M'-1} \tilde{\chi}^{0\dagger}_{a'_s b'_s} |vac\rangle \ ,$$

and for $(i,l),(k,j) \in \{(a'_s, b'_s)\}$:

$$\begin{aligned}\left[\tilde{\chi}^0_{ij}\,; \prod_{s=1}^{M'} \tilde{\chi}^{0\dagger}_{a'_s b'_s}\right] |vac\rangle &= \left[\tilde{\chi}^0_{ij}\,, \tilde{\chi}^{0\dagger}_{il}\tilde{\chi}^{0\dagger}_{kj}\right] \prod_{s=1}^{M'-2} \tilde{\chi}^{0\dagger}_{a'_s b'_s} |vac\rangle \\ &= \frac{1}{2}\tilde{\chi}^{0\dagger}_{kl} \prod_{s=1}^{M'-2} \tilde{\chi}^{0\dagger}_{a'_s b'_s} |vac\rangle \ .\end{aligned}$$

So, if the spins on sites i and j are paired in a singlet prior to the operation there is no change in in the singlet configuration, and the uncharged singlet is simply changed into a charged one. Else, the (uncharged) sites, $k \in A$ and $l \in B$ paired with i and j, respectively, forms a new uncharged singlet and a factor $1/2$ is also introduced.

In the case of operating onto two neighboring sites each carrying a charge so the $T^{(-)}_{rr'}$ terms are active, the treatment is slightly more complicated, and in the following the valence bond operators are not written out to clarify the action of the charge operators:

$$|\tilde{V}\rangle \doteq \prod_{s=1}^{M} \tilde{c}^\dagger_{a_s} \tilde{c}^\dagger_{b_s} |vac\rangle \ .$$

Again, the quasi singlets are affected analogous to ordinary spin. Consider $\tilde{c}_j\tilde{c}_i$ where where i and j matches two indices in $\{a_s\}$ and $\{b_s\}$. If these sites are found in the same charge decorated valence bond operator, $(i,j) \in \{(a_s, b_s)\}$, the result is found in a straight forward way:

$$\begin{aligned}\tilde{c}_j\tilde{c}_i |\tilde{V}\rangle &\doteq \tilde{c}_j\tilde{c}_i \left(\tilde{c}^\dagger_i\tilde{c}^\dagger_j \prod_{s=1}^{M-1} \tilde{c}^\dagger_{a_s}\tilde{c}^\dagger_{b_s}\right) |vac\rangle \\ &= \left[\tilde{c}_j\tilde{c}_i\,, \tilde{c}^\dagger_i\tilde{c}^\dagger_j\right] \prod_{s=1}^{M-1} \tilde{c}^\dagger_{a_s}\tilde{c}^\dagger_{b_s} |vac\rangle = \prod_{s=1}^{M-1} \tilde{c}^\dagger_{a_s}\tilde{c}^\dagger_{b_s} |vac\rangle \ ,\end{aligned}$$

as $\tilde{c}_j\tilde{c}_i$ commutates with the other charge operator pairs when no indices are matching i or j. Here, this operator acts like the identity operator in singlet space, and the result is that the specified singlet becomes charge-less.

$$\tilde{c}_j\tilde{c}_i\tilde{\chi}^{0\dagger}_{ij}\tilde{\chi}^0_{ij} |\tilde{V}\rangle = \prod_{s=1}^{M-1} \left(\tilde{c}^\dagger_{a_s}\tilde{c}^\dagger_{b_s}\tilde{\chi}^{0\dagger}_{a_s b_s}\right) \tilde{\chi}^{0\dagger}_{ij} \prod_{s=1}^{M'} \tilde{\chi}^{0\dagger}_{a'_s b'_s} |vac\rangle \ ,$$

[4]It should be understood that the factors removed from the product sequence correspond to the charge and valence bond operators containing the specified indices.

Now, consider the situation when the sites i and j are not in the same charged singlet, but paired with two other sites, k and l, i.e. $(i,l),(k,j) \in \{(a_s,b_s)\}$:

$$\tilde{c}_j\tilde{c}_i\,|\tilde{V}\rangle \doteq \tilde{c}_j\tilde{c}_i\left(\tilde{c}_i^\dagger\tilde{c}_l^\dagger\,\tilde{c}_k^\dagger\tilde{c}_j^\dagger\prod_{s=1}^{M-2}\tilde{c}_{a_s}^\dagger\tilde{c}_{b_s}^\dagger\right)|vac\rangle\ .$$

The factor $\tilde{c}_i\tilde{c}_i^\dagger$ gives one, and commutating $\tilde{c}_j$ past $\tilde{c}_l^\dagger\tilde{c}_k^\dagger$ gives a factor $(-1)^2 = 1$. However, the convention is to write the charge operators in AB pairs with the A and B site to the left and right, respectively, and a *sign flip* is introduced by commutating the charge operators $\tilde{c}_l^\dagger\tilde{c}_k^\dagger$ into the right order. So the full expression is:

$$\tilde{c}_j\tilde{c}_i\tilde{\chi}_{ij}^{0\dagger}\tilde{\chi}_{ij}^{0}\,|\tilde{V}\rangle = -\frac{1}{2}\tilde{c}_k^\dagger\tilde{c}_l^\dagger\tilde{\chi}_{kl}^{0\dagger}\prod_{s=1}^{M-2}\left(\tilde{c}_{a_s}^\dagger\tilde{c}_{b_s}^\dagger\tilde{\chi}_{a_sb_s}^{0\dagger}\right)\tilde{\chi}_{ij}^{0\dagger}\prod_{s=1}^{M'}\tilde{\chi}_{a'_sb'_s}^{0\dagger}\,|vac\rangle\ .$$

Again, the singlet part behaves as previously, pairing the i and j sites into one singlet and k and l into another, giving a factor $1/2$ and the combined amplitude is then $-1/2$.

4.2.2 Construction of the GS projection operator

Following the procedure from constructing the projector operator for the Heisenberg model, one first need a supremum estimation of the highest energy level in the charge decorated singlet sector, E_{HES}, to shift the spectrum appropriately. Such an estimation can be obtained by considering the largest possible individual contribution from each term in the Hamiltonian as operating on a corresponding two- or one-site eigenstate.

For the kinetic terms only one of $T_{ij}^{(-)}$ and $T_{ij}^{(+)}$ can be simultaniously active when acting on a state of some specific charge configuration, and an eigenstate must be written as an linear combination of two states, for which the $T_{ij}^{(+)}$ and $T_{ij}^{(-)}$ operates in a mirrored fashion. If the singlet projection gives a maximum factor of magnitude one, and neglecting any phase factors from the fermionic operators, one finds:

$$t\left(T_{ij}^{(+)}+T_{ij}^{(-)}\right)|\phi_{ij}\rangle = \lambda_{ij}^{(t)}\,|\phi_{ij}\rangle\ ,\quad \lambda_{ij}^{(t)} \le 2t\,,$$

and the number operator in the interaction term also gives a contribution of one:

$$Uh_i^{(U)}\,|\phi_i\rangle = \lambda_i^{(U)}\,|\phi_i\rangle\ ,\quad \lambda_i^{(U)} \le U/2\,,$$

so that a crude estimation, serving as an suitable spectrum shift constant $\tilde{C}$, would be:

$$E_{HES} \le \sum_{\langle i,j\rangle} 2t + \sum_i \frac{U}{2} \equiv \tilde{C}\,, \tag{4.2}$$

Now the Hamiltonian has to be put in a form that is compatible with the expansion of the GS projection operator into projection strings, which is done by rewriting each term as a AB nearest-neighbor interaction operator. The kinetic term is already in this form, and the interaction term becomes:

$$Uh_U = \frac{U}{2}\sum_i \tilde{n}_i = \frac{U}{2z}\sum_{\langle i,j\rangle}(\tilde{n}_i + \tilde{n}_j)\,.$$

It is suitable to add the eigenvalue spectrum shifting constant $\tilde{C}$ to the on-site interaction term, as it is also diagonal in character:

$$Uh_U - \tilde{C} = \sum_{\langle i,j\rangle}\left[\frac{U}{2z}\left(\tilde{n}_{ij} - 2\right) - 2t\right]\,, \quad \tilde{n}_{ij} = \tilde{n}_i + \tilde{n}_j\,,$$

and then, using the general expression for the ground state projecting operator (3.1), it is written[5]:

$$\begin{aligned}
\pi^{(k)} &\sim (-\tilde{\mathscr{H}} + \tilde{C})^k \\
&= \left(-2t\sum_{\langle i,j\rangle}(-1)^i \left(\frac{1}{4} - \boldsymbol{q}_i\cdot\boldsymbol{q}_j\right)(\tilde{c}_i^\dagger\tilde{c}_j^\dagger + \tilde{c}_j\tilde{c}_i) - \sum_{\langle i,j\rangle}\left[\frac{U}{2z}\left(\tilde{n}_{ij}-2\right) - 2t\right] \right)^k \\
&\sim \left(\sum_{\langle i,j\rangle}\tilde{Q}_{ij}(\tilde{c}_i^\dagger\tilde{c}_j^\dagger + \tilde{c}_j\tilde{c}_i) + \sum_{\langle i,j\rangle}\left[1 + \frac{U}{4zt}\left(2 - \tilde{n}_{ij}\right)\right]\right)^k\,,
\end{aligned}$$

and for finite k, the operator $\pi^{(k)}$ can be expanded as a sum of operator strings:

$$\pi^{(k)} \sim \sum_r P_r^{(k)}\,, \quad P_r^{(k)} = \coprod_{p=1}^{k} O^{(*)}_{i_p j_p}\,,$$

where the projector strings are simply sequences of the nearest-neighbor operators found in the Hamiltonian, with operators $O^{(*)}_{i_s j_s}$, acting on nearest-neighbor sites i_s and j_s are one of two *types*; either *off-diagonal* or *diagonal*, corresponding to a singlet-projection and charge-modifying term or a charge-counting term (including the eigenvalue shift constant) in a form as written in the ground state projection operator, respectively.

$$O^I_{ij} = \tilde{Q}_{ij}\left(\tilde{c}_i^\dagger\tilde{c}_j^\dagger + \tilde{c}_j\tilde{c}_i\right)\,, \quad O^{II}_{ij} = 1 + \frac{U}{4zt}\left(2 - \tilde{n}_{ij}\right)\,. \tag{4.3}$$

The action of the operator $O^I_{ij} = \frac{1}{2}\left(T^{(+)}_{ij} + T^{(-)}_{ij}\right)$ on the charged valence bond states is illustrated in figure 4.1.

[5] Again, one does not have to consider the normalization factor, as it cancels in the final expression used for calculating quantities of the ground state.

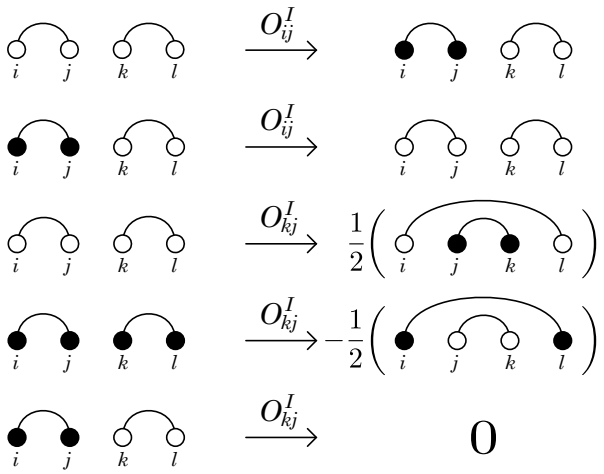

FIGURE 4.1: The action of the charge decorated singlet projection operator onto charged valence bond states, with O^I_{ij} defined in (4.3) and $i, k \in A$, $j, l \in B$.

By this construction, the operator $\pi^{(k)}$ projects out an approximate ground state from an arbitrary state for large k:

$$|GS\rangle \sim \sum_r P_r^{(k)} |\tilde{V}_0\rangle = \sum_r w_r |\tilde{V}_r\rangle \ ,$$

where w_r is a product of all the factors from the nearest-neighbor operators in the specific string obtained when applying it on the initial state, with each factor evaluated as described above.

4.2.3 An expression for the GSE

As before, the goal is to find an approximate value for the ground state energy level, and one may write:

$$E_0 = \frac{\langle\psi| \tilde{\mathscr{H}} \pi^{(k)} |\tilde{V}_0\rangle}{\langle\psi| \pi^{(k)} |\tilde{V}_0\rangle} = \frac{\sum_r w_r \langle\psi| \tilde{\mathscr{H}} |\tilde{V}_r\rangle}{\sum_r w_r \langle\psi|\tilde{V}_r\rangle} , \quad k \to \infty . \tag{4.4}$$

Here, one may choose $|\psi\rangle$ as a generalized quasi-spin Néel state decorated with quasi-charges.

Charge decorating the Néel state

Starting with an uncharged staggered quasi spin state $|\Psi_N\rangle$, one may form a linear combination of states, consisting of *charge decorated Néel states* corresponding to all possible charge configurations on the lattice compatible with

the restriction of balanced sub-lattice charge density:

$$|\tilde{\Psi}_N\rangle = \sum_{C.C.} \left(\prod_p \tilde{c}^\dagger_{a_p} \tilde{c}^\dagger_{b_p} |\Psi_N\rangle \right) .$$

The AB-site pairs, (a_p, b_p), of the charge operators $\tilde{c}^\dagger_{a_p}\tilde{c}^\dagger_{b_p}$ giving a specific charge configuration in the extended Néel state are defined such that

$$a_1 < a_2 < \ldots < a_n , \quad b_1 < b_2 < \ldots < b_n .$$

The overlap for all charge decorated valence bond states as in (4.1) are then equal up to a sign from the contraction of the charge operators defining the projected state and the corresponding term in the Néel state with matching charge configuration. As noted above, the sequence of charge operator pairs, $\{(\tilde{c}^\dagger_{a'_p}, \tilde{c}^\dagger_{b'_p})\}$, defining the charge state of $|\tilde{V}\rangle$ may unambiguously be ordered so that $a'_p = a_p$ holds. The sequence $\{b'_p\}$ is then defined by this order:

$$\begin{aligned}\langle\tilde{\Psi}_N|\tilde{V}\rangle &= \langle\Psi_N|\, \tilde{c}_{b_n}\tilde{c}_{a_n} \ldots \tilde{c}_{b_2}\tilde{c}_{a_2}\tilde{c}_{b_1}\tilde{c}_{a_1}\tilde{c}^\dagger_{a_1}\tilde{c}^\dagger_{b'_1}\tilde{c}^\dagger_{a_2}\tilde{c}^\dagger_{b'_2}\ldots\tilde{c}^\dagger_{a_n}\tilde{c}^\dagger_{b'_n}\,|V\rangle \\ &= \langle\Psi_N|\, \tilde{c}_{b_n}\ldots\tilde{c}_{b_2}\tilde{c}_{b_1}\,\tilde{c}^\dagger_{b'_1}\tilde{c}^\dagger_{b'_2}\ldots\tilde{c}^\dagger_{b'_n}\,|V\rangle = (-1)^m \left(1/\sqrt{2}\right)^{N/2} .\end{aligned}$$

The sign of the overlap is determined by commutating the operator sequence $\tilde{c}^\dagger_{b'_1}\ldots\tilde{c}^\dagger_{b'_n}$ into increasing order with regards to their index labels, with m being the number of operator-pair commutations (i.e. $\tilde{c}^\dagger_b\tilde{c}^\dagger_{b'} = -\tilde{c}^\dagger_{b'}\tilde{c}^\dagger_b$) required to do so.

Although the generalized Néel state of this construction has non-zero overlap of each individual CDVB, it can not be guaranteed that the total overlap of the projected ground state does not vanish. However, for small t/U, the ground state should be found as a perturbation of the uncharged valence bond state from the Heisenberg model with only small amplitudes for the charged basis states, giving a sizable overlap.

A sampleable expression

Putting the Hamiltonian in a form of nearest-neighbor terms (4.3):

$$\tilde{\mathscr{H}} = -2t \left[\sum_{\langle i,j\rangle} O^I_{ij} + \sum_{\langle i,j\rangle} \left(O^{II}_{ij} - \frac{\tilde{C}_{ij}}{2t} \right) \right] , \quad \frac{\tilde{C}_{ij}}{t} = 2 + \frac{U}{zt} ,$$

and using the charge decorated Néel state, one can rewrite the overlaps found in the expression for E_0 (4.4) :

$$\begin{aligned}\langle\tilde{\Psi}_N|\,\tilde{\mathscr{H}}\,|\tilde{V}_r\rangle &= t\sum_{\langle i,j\rangle} h^{(r)}_{ij}\,\langle\tilde{\Psi}_N|\tilde{V}^{(ij)}_r\rangle = t\sum_{\langle i,j\rangle} h^{(r)}_{ij}\eta^{(r)}_{ij}|\,\langle\tilde{\Psi}_N|\tilde{V}^{(ij)}_r\rangle\,| , \\ \langle\tilde{\Psi}_N|\tilde{V}_r\rangle &= \eta_r|\,\langle\tilde{\Psi}_N|\tilde{V}_r\rangle\,| ,\end{aligned}$$

with h_{ij} evaluated as for the corresponding operators[6] $-2O^I_{ij}$, $(-2O^{II}_{ij}+\tilde{C}_{ij}/t)$, and the sign function:

$$\eta = \frac{\langle\tilde{\Psi}_N|\tilde{V}\rangle}{|\,\langle\tilde{\Psi}_N|\tilde{V}\rangle\,|}\,.$$

Then the ground state can be written:

$$E_0 = \frac{\sum_r w_r\left(t\sum_{\langle i,j\rangle} h^{(r)}_{ij}\eta^{(r)}_{ij}|\,\langle\tilde{\Psi}_N|\tilde{V}^{(ij)}_r\rangle\,|\right)}{\sum_r w_r\left(\eta_r|\,\langle\tilde{\Psi}_N|\tilde{V}_r\rangle\,|\right)} = \frac{\sum_r w_r\left(t\sum_{\langle i,j\rangle}\eta^{(r)}_{ij}h^{(r)}_{ij}\right)}{\sum_r w_r\eta_r}\,.$$

The sign problem

The expansion coefficients in terms of the individual contribution from each projection string can not be argued to be positive definite in the same way as in the case of projecting out the Heisenberg ground state in the ordinary valence bond basis. This is so when an odd number of off-diagonal operators in a projection string give each gives a factor $-1/2$ as shown above, and thus the amplitudes for some propagated states are negative. This becomes a problem when these amplitudes are intended to be used as a statistical weight, and is called *the sign problem*.

One may then consider a *reweighted* sampling process, where some positive function $W_r(w_r)$ is defined and serves as a weight in an importance sampling of a *virtual system*, defined by these modified weights and a corresponding modified estimator of the quantity sampled. Using the standard $W_r = |w_r|$, and introducing a factor one as $\sum_r|w_r|/\sum_r|w_r|$, one obtains:

$$E_0 = \frac{\sum_r|w_r|\frac{w_r}{|w_r|}\left(t\sum_{\langle i,j\rangle}\eta^{(r)}_{ij}h^{(r)}_{ij}\right)}{\sum_r|w_r|\frac{w_r}{|w_r|}\eta_r}\cdot\frac{\sum_r|w_r|}{\sum_r|w_r|} = \left[\frac{\sum_r|w_r|v_r}{\sum_r|w_r|}\right]\Big/\left[\frac{\sum_r|w_r|s_r}{\sum_r|w_r|}\right]\,,$$

where

$$v_r = \frac{w_r}{|w_r|}\left(t\sum_{\langle i,j\rangle}\eta^{(r)}_{ij}h^{(r)}_{ij}\right)\,,\quad s_r = \frac{w_r\eta_r}{|w_r|}\,.$$

Here, an expression for the ground state energy is found as a quotient of two weighted sums, the *virtual energy* and *negative sign ratio* respecively:

$$\frac{E_0(t/U)}{t} = \frac{e_v/t}{s_v}\,,\quad e_v/t = \frac{\sum_r|w_r|(v_r/t)}{\sum_r|w_r|}\,,\ s_v = \frac{\sum_r|w_r|s_r}{\sum_r|w_r|}\,,$$

both individually interpretable as statistical expectation values in the sense that the modified weights are positive definite. The ground state energy of the T_0-less Hubbard model on a specific lattice can then be calculated for some choice of t/U by sampling both these estimators over the contributing projection strings, using the weight $|w_r|$ in the importance sampling scheme.

[6] Note that the energy parameters t and U only appear here in the form t/U.

4.2.4 Updating the projection strings

In the simulation of the HB-model using Projector QMC in the VB-basis, the simplistic algorithm that was used to generate new trial projection strings was very efficient. The trial strings were generated by randomly changing which neighboring pair of sites a number of projection operators in the projection string was acting on, with the permuted operators and their respective translation selected uniformly. Any projector string generated in this way would have a non-zero weight in the importance sampling, as no operator could annihilate any valence bond state.

In this model with operators in the Hamiltonian introducing charge fluctuations, unfortunately also introduce the possibility of *killing* a quasi-charged VB-state with a *misplaced* quasi-charge operator. This happens when an off-diagonal operator, O^I_{ij}, in a projector string acts on a pair of sites, (i,j), in an intermediate state where only one of the sites is occupied by a quasi-charge. Such particular string has zero weight in the importance sampling, i.e. represent an *unimportant* projector string. This fact makes a huge impact on the probability of generating valid (non-zero weight) projection strings using a the simplistic updating algorithm as the one used in the simulation of the HB-model. This is so as the only way of inserting (or removing) a *single* off-diagonal operator acting on a neighboring site-pair, $T^{(\pm)}_{ij}$, into (or from) a non-zero weight projection string, is if all later off-diagonal operators in the string acting on any site of this specific pair of sites only operate on both sites. This effectively suppresses all attempts of updates involving $T^{(\pm)}_{ij}$ early in the projection string, where the probability of an incompatible off-diagonal operator later in the string is large.

Not being able to make updates of the off-diagonal operators early in the projection string is a major issue, as efficiency in the sampling is very low when most string generated are given weight zeros, and further the length of the valid strings are effectively capped by this. The first part of the trial string can be said to be static in terms of off-diagonal operators, and effectively only serves as providing a random initial CDVB-state for sampling in the latter part. To make Projector QMC work in this model then demands a better scheme of generating the trial projector strings, which do not have the problem of having an effective maximum projector string length.

Operator-loop updates

To remedy this one may consider an *operator-loop* update scheme, which is constructed to handle this delicate structure of the quasi-charge operators in the projection strings in a better way[7]. The idea of an operator-loop updating

[7] Although no proof can be provided, experience from extensive simulations strongly suggest that the operator-loop updates does not generate any non-valid projector strings.

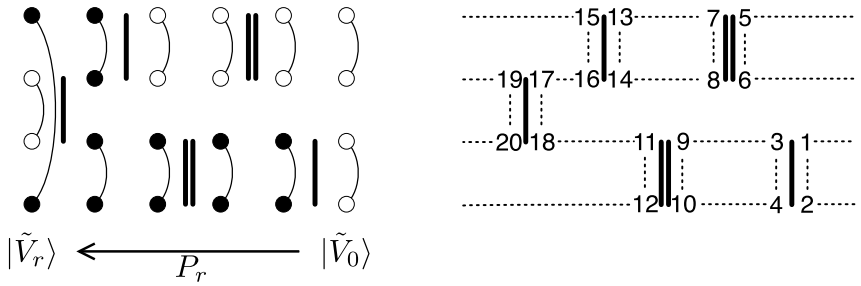

(a) State propagation (b) Loop structure

FIGURE 4.2: The propagation of a four-site CDVB during application of a projection string P_r ($k = 5$) with the intermediate states (with amplitudes and phase factors neglected). Off-diagonal operators are represented by a single line marking the sites on which they are operating, and diagonal operators with double lines. The operator loop structure formed by this projection string is also illustrated, with leg labels q written out.

scheme formulated here to handle the charge-decorated operators is inspired by the loop-updates for valence-bond PMC as presented in [14].

As noted, the updating generally fails when an off-diagonal operator is introduced or removed from the string, as after the update this or other *downstream* off-diagonal operators may happen to be acting on a mixed charge state. Considering a single operator in the operator string and the nearest-neighboring pair onto which it operates, one may track and form a list of all the operators acting onto the lattice sites in question. Changing this specific operator could only affect the operators found in this list, however the same operator might be found in more than one list, if a corresponding list is formed for each operator in the string. The basic idea of the operator-loop update is now to find (limited) sets of operators connected through these lists such that the operators in a set can be simultaneously updated, yielding a valid projector string.

To this end, one may construct a *loop structure*, containing information on which operators may affect which other operators in a specific update through the intermediate charge states they act onto. In the following refer to figure 4.2. Constructing the operator-loop structure is done by assigning each *leg* of each operator in the string a label as $q = 4(p-1)+l$, with p being the position of the operator in the string, and $l = \{1, 2, 3, 4\}$ is the internal numbering of the four legs of each operator. Thus $1 \leq q \leq 4k$, for a string of length k. The complete string is then transversed and a list is formed by noting which leg is *connected* to each leg of each operator. If also the *upstream* and *downstream* legs of an operator are said to be connected, an *operator loop* can then be traced out by starting with an arbitrary operator leg and following these connections between legs, noting which operators are forming the loop as one goes along.

The actual update of the projection string consists of two distinct modes, of

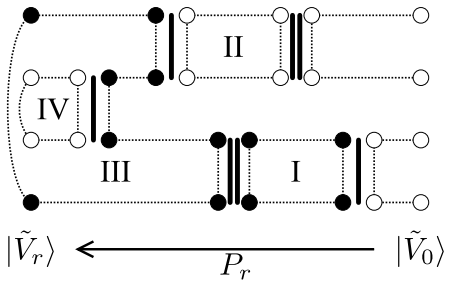

FIGURE 4.3: The closed loops formed by the projection string from figure 4.2, with the affected charge states shown but the valence bonds left out for readability. All four operator loops found in this example are flippable.

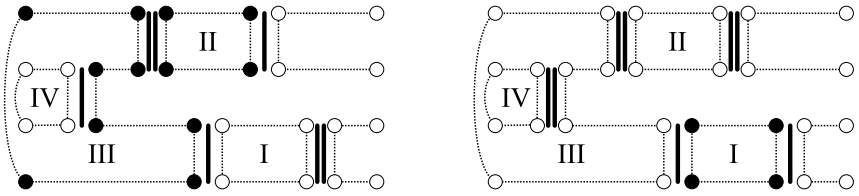

(a) Loops I and II flipped

(b) Loop III flipped

FIGURE 4.4: The projection strings and charge states obtained when performing type-flip loop updates on the projection string from figure 4.2 and 4.3.

which one is randomly chosen for each update of the sampling process. The first is similar to the trivial random translation update as in the simulation of the HB model, but here only the diagonal operators in the string are considered. This poses no problem, as by (4.3) these operators always has a non-zero eigenvalue for every possible configuration. The second is the actual loop update, where the loop structure of the projection string is used (figure 4.3). It can be observed that if the type of each operator connected to an operator-loop is *flipped*, meaning $O^I_{ij} \to O^{II}_{ij}$ and $O^{II}_{ij} \to O^I_{ij}$, the charge state outside of the loop will be preserved. Assuming the original string is valid, no off-diagonal operator in the string downstream of the updated loop will then risk killing the propagating state. Thus, the update consists of *type-flipping* each operator loop found in the string with some probability, as in figure 4.4.

Loop-flip updates where any diagonal operator operating on a mixed charge state is to be flipped are excluded, as this update would kill the propagation inside the loop. Charge fluctuations in the projected state is introduced by the interpretation that an *open operator loop* connected to the projected state is to be considered to be closed (through an unspecified hypothetical continuation of the loop structure downstream of the projected state) and is allowed to be flipped. Loops similarly connected to the initial state are however excluded, as the initial state is to be kept fixed throughout the sampling.

Ergodicity of the sampling scheme

In both update modes described above, there is a non-zero probability of suggesting a trivial update, implying that the Markov chain of string configurations is non-periodical. One may also find that all contributing string configurations are connected by at least one specific updating sequence. Observing that it is possible to remove all off-diagonal operators from any projector string one-by-one by translating the diagonal operators such that none are acting on the sites of the last off-diagonal operator. Then the open loop formed by this off-diagonal operator and the projected state can be flipped, changing the off-diagonal operator to the corresponding diagonal one. Repeating this procedure for all off-diagonal operators, the string can be reduced to a string consisting of only diagonal operators. Since the procedure outlined is reversible in each step, it is also possible to construct any valid string configuration from a string of diagonal operators. As all such reduced strings are trivially connected by translation updates, one can conclude that the Markov chain is also irreducible. Thus, the sampling scheme is ergodic.

The candidate generating functions in both update modes described above are symmetrical. The translation of diagonal operators trivially so, and also the loop-update as the loop structure is preserved in a loop-flip update. With the standard acceptance probability $p_{acc} = \min(w'/w, 1)$, detailed balance is satisfied, and the limit distribution density in the generated Markov chain of string configurations becomes proportional to the (modified) weights of the strings.

Details of the implementation

As for PMC in the Heisenberg model, a set of convergence runs are first performed for each lattice and value of t/U to find a suitable projector string length, k. To obtain reasonable acceptance rates, the parameters of the updating algorithm is tuned to reduce the number of operators changed in the projection string for small values of t/U. This is because the weight of the projection strings may differ substantially by even very small changes when the range of the diagonal operators diverge as $t/U \to 0$. Here, the number of operators affected by the translation-mode update is set $\sim t/U$ and the probability of type-fipping a valid operator loop in the loop-mode update $\sim t/U \cdot n_l^{-1}$, where n_l is the number of operators in the loop considered.

4.3 Variational expressions

When forming an expression for the ground state expectation value of arbitrary operators, similar to the expression (3.8) in the ordinary valence bond basis, it is not trivial to find an effective sampling scheme. This issue arises from

the fact that the charge decorated valence bond states are *mostly orthogonal*, and only states with matching charge configurations have non-zero overlap. A formal expression can be written:

$$\begin{aligned}\langle \mathscr{A} \rangle_{GS} &= \frac{\sum_{l,r} \langle \tilde{V}_0' | \, P_l^\dagger \mathscr{A} P_r \, | \tilde{V}_0 \rangle}{\sum_{l,r} \langle \tilde{V}_0' | \, P_l^\dagger P_r \, | \tilde{V}_0 \rangle} = \frac{\sum_{l,r} w_l w_r \, \langle \tilde{V}_l | \, \mathscr{A} \, | \tilde{V}_r \rangle}{\sum_{l,r} w_l w_r \, \langle \tilde{V}_l | \tilde{V}_r \rangle} \\ &= \left[\frac{\sum_{l,r} |w_l w_r| \left(\frac{w_l w_r}{|w_l w_r|} \, \langle \tilde{V}_l | \, \mathscr{A} \, | \tilde{V}_r \rangle \right)}{\sum_{l,r} |w_l w_r|} \right] \Bigg/ \left[\frac{\sum_{l,r} |w_l w_r| \left(\frac{w_l w_r}{|w_l w_r|} \, \langle \tilde{V}_l | \tilde{V}_r \rangle \right)}{\sum_{l,r} |w_l w_r|} \right] .\end{aligned}$$

As the expression is written, one should sample over the pairs of projection strings with non-zero individual weight w_i. However, only a few of these pairs will have a non-zero overlap, and thus the divisor will tend to be very small, leading to increased statistical inaccuracies of the quantity calculated. Also, the matrix elements $\langle \tilde{V}_l | \, \mathscr{A} \, | \tilde{V}_r \rangle$ are typically only non-zero for a small fraction of left and right states (e.g. the Hamiltonian). One might be able to effectively sample such operators by constructing an updating algorithm that discards non-contributing configuration pairs.

However, for operators satisfying

$$\langle \tilde{V}_l | \tilde{V}_r \rangle = 0 \quad \Rightarrow \quad \langle \tilde{V}_l | \mathscr{A} | \tilde{V}_r \rangle = 0 \, ,$$

for all combinations of left and right projection strings (e.g. operators diagonal in charge space), one may include the overlap in the weight and form the expression:

$$\langle \mathscr{A} \rangle_{GS} = \left[\frac{\sum_{l,r} W_{l,r} \, (\eta_{l,r} a_{l,r})}{\sum_{l,r} W_{l,r}} \right] \Bigg/ \left[\frac{\sum_{l,r} W_{l,r} \eta_{l,r}}{\sum_{l,r} W_{l,r}} \right] ,$$

with

$$W_{l,r} = |w_l w_r \, \langle \tilde{V}_l | \tilde{V}_r \rangle \, | \, , \quad \eta_{l,r} = \frac{w_l w_r \, \langle \tilde{V}_l | \tilde{V}_r \rangle}{|w_l w_r \, \langle \tilde{V}_l | \tilde{V}_r \rangle \, |} \, , \quad a_{l,r} = \frac{\langle \tilde{V}_l | \, \mathscr{A} \, | \tilde{V}_r \rangle}{\langle \tilde{V}_l | \tilde{V}_r \rangle} \, .$$

The sampling can in this case be restricted to projection string pairs, $P_l \, , P_r$, resulting in states with non-zero overlaps. The operator loop scheme can accommodate this with minor adaptions, by updating both left and right projection string as if they where concatenated into one string of double length, $P_{l,r} = P_l^\dagger P_r$.

4.4 Results for the T_0-less model

Simulations where performed on small 1D chains, with sizes ranging from $L = 6$ to $L = 12$, calculating the ground state energies for the T_0-less Hubbard model of these systems. Table 4.1 contains calculated values of per-site $E_0 = e_v / s_v$

TABLE 4.1: Calculated E_0 compared to exact values.

L	t/U	$E_0^{(PMC)}/tL$	E_0/tL	$\Delta E/E_0$	k	e_v/tL	s_v
	1/16	-0.172 ± 0.021	-0.1741	$+0.012$		-0.168 ± 0.022	0.976 ± 0.003
	1/8	-0.327 ± 0.010	-0.3236	-0.009		-0.303 ± 0.010	0.924 ± 0.004
6	1/4	-0.528 ± 0.005	-0.5343	$+0.011$	$8L$	-0.437 ± 0.003	0.828 ± 0.005
	1/2	-0.750 ± 0.005	-0.7506	$+0.001$		-0.548 ± 0.003	0.730 ± 0.003
	1	-0.913 ± 0.006	-0.9153	$+0.002$		-0.613 ± 0.003	0.671 ± 0.004
	1/16	-0.180 ± 0.017	-0.1715	-0.047		-0.174 ± 0.018	0.966 ± 0.002
	1/8	-0.321 ± 0.013	-0.3186	-0.006		-0.292 ± 0.012	0.908 ± 0.003
8	1/4	-0.524 ± 0.007	-0.5237	-0.001	$7L$	-0.422 ± 0.006	0.805 ± 0.005
	1/2	-0.724 ± 0.007	-0.7275	-0.003		-0.495 ± 0.004	0.683 ± 0.004
	1	-0.877 ± 0.012	-0.8775	$+0.001$		-0.504 ± 0.004	0.575 ± 0.006
	1/16	-0.172 ± 0.013	-0.1697	-0.012		-0.164 ± 0.013	0.954 ± 0.003
	1/8	-0.324 ± 0.008	-0.3153	-0.029		-0.287 ± 0.008	0.886 ± 0.006
12	1/4	-0.523 ± 0.004	-0.5188	-0.008	$5.75L$	-0.408 ± 0.003	0.781 ± 0.004
	1/2	-0.723 ± 0.010	-0.7229	-0.000		-0.480 ± 0.005	0.664 ± 0.007
	1	-0.873 ± 0.013	-0.8754	-0.002		-0.492 ± 0.004	0.564 ± 0.007

over a range of relative interaction strengths $1/16 \leq t/U \leq 1$ obtained by the PMC method presented in this chapter, and these values is compared to the energy obtained using the *Lanczos algorithm* as presented in Appendix B. Similar to the Heisenberg model, the per-site ground state energy is decreasing for larger system size with t/U fixed.

As before, the error estimation is given the standard deviation of independent walkers for each set of simulation parameters, as performing a binning-type error estimation is rather involving for non-linear quantities [15]. Here, $n_{MCS} = 4 \cdot 10^5 k$ is used, and as seen in table 4.1 and figure 4.5, the error is increased for small t/U. This can be attributed to the issue of vanishing acceptance rates in the sampling. Then correlation of the sampled configurations are increased, effectively reducing the number of samples form the simulation run yielding the estimated E_0, suggesting one could consider a t/U-dependent scaling parameter, $n_{MCS} \sim k^{\gamma_n(t/U)}$. To reduce the computational load of the simulation for the larger systems, $k \sim N^{1/2}$ is chosen, but then the estimated E_0 seems to be consistently lower than the exact value for $L = 8, 12$, and more so for small t/U. Thus, also the scaling of the projection string length should be adjusted with t/U, setting $k = N^{\gamma(t/U)}$.

With the scalings used in the simulations running time is linear in N, and the time spent for each run for $L = 12$ is just over one hour with a single-CPU computer. However, results strongly suggest a more costly scaling should be used, at least in simulations for small values of t/U.

Comparing with the Heisenberg and Hubbard models

In figure 4.6(a), exact and calculated values of $E_0(t/U)$ for $L = 6$ are presented along with exact results for the complete Hubbard model and the Heisenberg model. Here one can see how the ground state is split up away from $t/U \ll 1$ in

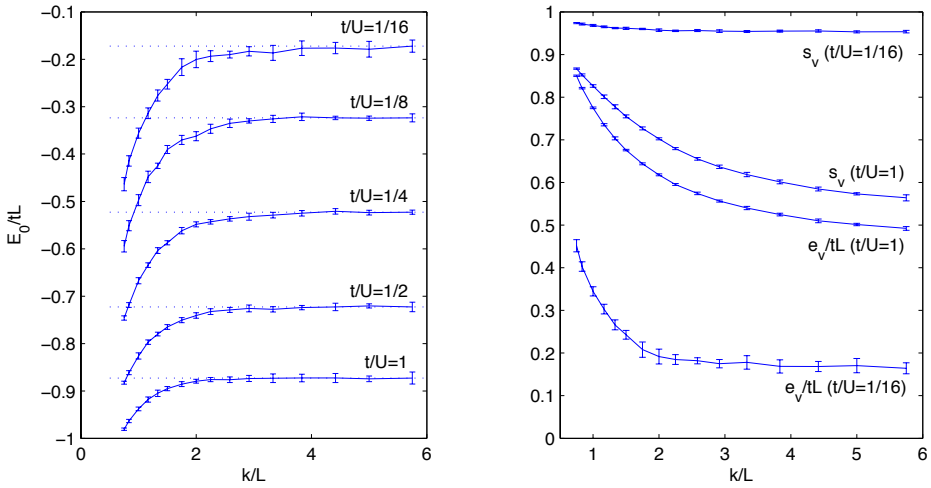

(a) Convergence of $E_0(t/U)$ in k, $L = 12$. (b) Convergence of $e_v(t/U)$ and $s_v(t/U)$ in k.

FIGURE 4.5: Convergence runs of $E_0(t/U)$ for $L = 12$. Here, $4 \cdot 10^5\, k$ samples are considered for each data point, divided over 10 walkers. Note that the ratio e_v/s_v yielding the ground state approximation may converge in k before e_v and s_v do so individually.

the models considered, and the effect of the on-site interaction energy penalty for the charge-fluctuating systems is considerable as t/U grows.

In figure 4.6(b) the *convergence rate parameter*, is plotted for $0 \leq t/U \leq 1$. It is the ratio of the first excited energy in the sampled sector, E_{FES} and E_0 that determines the rate of convergence for the ground state projection operator $\pi^{(k)}$. Including the spectrum shift constant $\tilde{C}$ from (4.2), the error in norm for the projection follow:

$$\epsilon^{(k)} \sim \left(\frac{E_{FES} - \tilde{C}}{E_0 - \tilde{C}} \right)^k$$

As can been seen, the ratio approaches 1 for $t/U \to 0$, reducing efficiency of the projection for small t/U. This can be contrasted by the corresponding ratio for the Heisenberg model for a 6-site 1D chain, which is found to be 0.70. Replacing this estimation, and using the exact value of E_{HES} as shift constant slightly increases the rate of convergence, but the ratio still approaches 1 as $t/U \to 0$. This is because the shifting constant diverges:

$$\tilde{C} \geq E_{HES} \sim U/t \to \infty\,, \quad t/U \to 0\,,$$

and then the shifted energy gap vanish for small t/U, as the unshifted E_0 and E_{FES} converges to the (bounded) values found in the corresponding Heisenberg model in this limit.

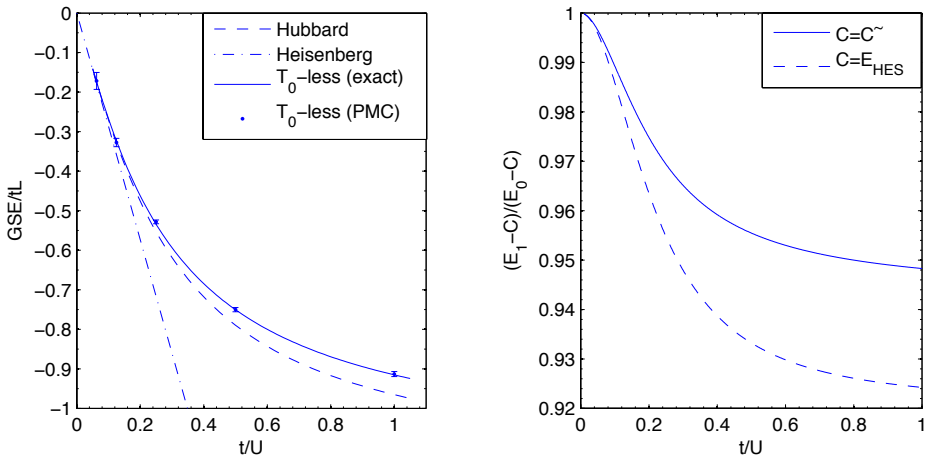

(a) Ground state energy, $L = 6$.

(b) Convergence rate parameter.

FIGURE 4.6: Per-site ground state energies of the Heisenberg, the complete and T_0-less Hubbard models for a 1D chain of 6 sites. The ratio determining the rate of convergence for the ground state projection operator is plotted for the spectrum shift constant used in the simulations $\tilde{C}$, and compared to the ratio obtained when the shift is set exactly to E_{HES}.

An effective kinetic energy

Considering how remarkably close the energy for the T_0-less model follow the complete Hubbard model, it may be tempting to try *fudging* the parameters to make calculations of $E_0(t/U)$ in the T_0-less model useful as estimations of the complete Hubbard model. This may be done by scaling the t in the T_0-less Hamiltionian:

$$\tilde{\mathscr{H}}(t,U) = t(T_+ + T_-) + Uh_U \quad \rightarrow \quad \tilde{\mathscr{H}}'(t,U) = \alpha t(T_+ + T_-) + Uh_U\,,$$

replacing t with an *effective value*, aiming to compensate for the missing hopping mode associated with the T_0-term. Now E_0' for this modified Hamiltonian can be obtained by considering:

$$\frac{\tilde{\mathscr{H}}'(t,U)}{t} = \alpha(T_+ + T_-) + U/t\, h_U = \alpha\left(T_+ + T_- + \frac{U}{\alpha t}h_U\right) = \alpha\left(\frac{\tilde{\mathscr{H}}(\alpha t, U)}{\alpha t}\right),$$

Now let $\alpha = (1 + \beta t/U)$ and set $\beta = 0.058$, then the estimate

$$\frac{E_0'(t/U)}{t} = \alpha\left(\frac{E_0(\alpha t/U)}{\alpha t}\right)$$

differ by $\lesssim 1.5\%$ compared to the exact Hubbard ground state energy over $0 \leq t/U \leq 1$ for a 6 site chain, a more than three-fold improvement from the un-fudged T_0-less model in this range.

Chapter 5

Conclusions

The method of projection quantum Monte Carlo simulations in the valence bond basis combine the two very attractive qualities of simplicity and efficiency. However, the impressive results from the projector Monte Carlo simulations in the Heisenberg model was unfortunately not reflected in the results of the adapted T_0-less Hubbard model. This may in part be attributed to the issues stemming from the unfortunate energy spectrum of this model, but the more involved and time-consuming procedures for evaluating the weights and generating trial projection strings also affect the performance of this method and prevent simulating systems of larger sizes. The results presented for this T_0-less model have too large errorbars for precise readings of E_0 with the modest running time invested, but they do give indications on how the PMC algorithm scales for this type of system. Finding more accurate values is then a matter of having devotion and resources available.

Future work

The concepts and notions for PMC simulations of the T_0-less Hubbard model formulated in this work are not constrained to being only applicable to 1D systems. In fact, simulations in 2D (or higher dimensions) are readily implementable by the same method. For this to be practically feasible however, efficiency of the implementation must be significantly improved.

By implementing an efficient method of generating suitable initial states for subsequent ground state projection, the projection string length required can be reduced significantly [7, 8]. In the referenced work, an iterative algorithm is used to generate *self-optimized* valence bond states with a valence bond-length distribution similar to the projected approximate ground state, which is shown to to make excellent improvements in the efficiency of the projection in the Heisenberg model. A similar method might be applicable for the T_0-less model, improving the rudimentary method of pre-projection.

Appendix A

The Tight-binding model and Wannier states

If one pictures the process of forming a crystal as bringing together isolated atoms into a lattice, a one-electron Hamiltonian can be written as the atomic Hamiltonian of one atom, plus a correction generated from the potentials of all the surrounding ions in the lattice:

$$\mathscr{H}(\boldsymbol{r}) = \mathscr{H}_{atom}(\boldsymbol{r}) + \delta U(\boldsymbol{r})\,,$$

If the correction can be considered small, an approximate one-electron eigenfunction can be written as a linear combination of atomic eigenfunctions (orbitals) $\phi(\boldsymbol{r} - \boldsymbol{r}_j)$ of the isolated atomic Hamiltonians for each lattice site [16].

$$\psi_{\boldsymbol{k}}(\boldsymbol{r}) = \sum_j C_{\boldsymbol{k},j}\phi(\boldsymbol{r} - \boldsymbol{r}_j) = \frac{1}{\sqrt{N}}\sum_j \exp(i\boldsymbol{k}\cdot\boldsymbol{r}_j)\phi(\boldsymbol{r} - \boldsymbol{r}_j)\,, \tag{A.1}$$

where the particular form of writing the coefficients $C_{k,j}$ is chosen so that the wave function satisfies the Bloch condition. The expression to evaluate when calculating the energy of a crystal state of a specific $\boldsymbol{k}$ is:

$$\epsilon_{\boldsymbol{k}} = \frac{\langle \boldsymbol{k}|\mathscr{H}|\boldsymbol{k}\rangle}{\langle \boldsymbol{k}|\boldsymbol{k}\rangle}$$

with:

$$\langle \boldsymbol{k}|\mathscr{H}|\boldsymbol{k}\rangle = \frac{1}{N}\sum_{j,m}\langle \phi_m|\mathscr{H}|\phi_j\rangle \exp(i\boldsymbol{k}\cdot(\boldsymbol{r}_j - \boldsymbol{r}_m))$$

$$\langle \boldsymbol{k}|\boldsymbol{k}\rangle = \frac{1}{N}\sum_{j,m}\langle \phi_m|\phi_j\rangle \exp(i\boldsymbol{k}\cdot(\boldsymbol{r}_j - \boldsymbol{r}_m))\,.$$

A.1 Tight-binding Hamiltonian

In the tight-binding model, it is assumed that the overlap of the orbitals is small, and the only non-zero off-diagonal matrix elements in the Hamiltonian connects neighboring states [16]:

$$\begin{aligned} \langle \phi_j | \mathscr{H} | \phi_j \rangle &= -E_0 \\ \langle \phi_m | \mathscr{H} | \phi_j \rangle &= -\Delta\,, \quad m, j : |\boldsymbol{r}_m - \boldsymbol{r}_j| = a \\ \langle \phi_m | \phi_j \rangle &= \delta_{m,j}\,. \end{aligned}$$

If $\boldsymbol{\rho}_n$ is such a vector connecting a site to a nearest neighboring site, the expression for the energy can be written:

$$\epsilon_{\boldsymbol{k}} = -E_0 - \Delta \sum_n \exp(-i\boldsymbol{k}\cdot\boldsymbol{\rho}_n)\,.$$

A.2 Wannier functions

The Wannier functions of a particular band, are defined as [16]:

$$w(\boldsymbol{r} - \boldsymbol{r}_j) = \frac{1}{\sqrt{N}} \sum_{\boldsymbol{k}} \psi_{\boldsymbol{k}}(\boldsymbol{r}) \exp(-i\boldsymbol{k}\cdot\boldsymbol{r}_j)\,,$$

where the sum is over all the wave vectors in the first Brillouin zone compatible with the crystal volume, with associated wave function $\psi_{\boldsymbol{k}}(\boldsymbol{r})$. One finds that the Wannier functions are orthogonal and often peaked around the associated lattice site, $\boldsymbol{r}_j$. A wave function in this band can then be written

$$\psi_{\boldsymbol{k}}(\boldsymbol{r}) = \sum_j w(\boldsymbol{r} - \boldsymbol{r}_j) \exp(i\boldsymbol{k}\cdot\boldsymbol{r}_j)\,,$$

and comparing this form to the one-electron wave function for the tight binding model (A.1), one concludes that the Wannier functions are here approximated by the atomic orbitals.

Appendix B

Exact diagonalization of 1D spin systems

When constructing approximative calculation schemes such as PMC, it can be very helpful to have dependable results from more traditional (but slower) methods available for comparison and evaluation. Although these results may only be available for small systems or in some restricted range of the parameters, they may offer good value as a testing ground when identifying problems and finding bugs in the implementation of new methods.

B.1 Heisenberg model

For the Heisenberg model in 1D there are exact analytical solutions available for infinite spin chains through use of the celebrated *Bethe anzats*, which also can be generalized to the Hubbard model [17]. Here, a simplistic numerical method is presented for finding the ground state energy of a finite periodic spin chain of an even number of sites.

For a L-site spin-1/2 chain, one may use a basis of specific spins per site:

$$|\phi\rangle = |s_1, s_2 \dots s_L\rangle \ , \quad s_i = \uparrow \text{ or } \downarrow ,$$

and the Hamiltonian is written:

$$\begin{aligned} \mathscr{H} &= J \sum_i \left(\boldsymbol{S}_i \cdot \boldsymbol{S}_{i+1} - \frac{1}{4} \right) \\ &= \frac{J}{2} \sum_i \left(2 S_i^z S_{i+1}^z - \frac{1}{2} \right) + \left(S_i^+ S_{i+1}^- + S_i^- S_{i+1}^+ \right) \equiv \frac{J}{2} \sum_i H_{i,i+1} \, . \end{aligned}$$

One sees that the terms are only non-zero when operating on two adjacent anti-parallel spins, where one the action is diagonal (with eigenvalue -1) or

flips the spins in the state:

$$H_{i,i+1}\,|\ldots s_i, s_{i+1}\ldots\rangle = \begin{cases} -\,|\ldots s_i, s_{i+1}\ldots\rangle + |\ldots s_{i+1}, s_i\ldots\rangle\,, & s_{i+1} = -s_i \\ 0\,, & s_{i+1} = s_i\,. \end{cases}$$

The approach now is simply to go through all the basis states, apply the Hamiltonian and collect the results, building a matrix representation of the Hamiltonian column by column in this way. To do this one must *label* the basis states in such way that both *encoding* (i.e. finding the proper label for a specific spin configuration) and *decoding* (the reverse process) is efficient. Representing a state by a binary string of the same length as the spin chain is useful for this, and the the label of a state $|\phi\rangle$ is given by the integer interpretation of this binary string:

$$I_\phi = \sum_{i=1}^{L} b_i 2^{i-1}\,, \quad \text{where } b_i = \begin{cases} 1\,, & s_i = \uparrow \\ 0\,, & s_i = \downarrow \end{cases}.$$

This representation of the states is convenient, as bit manipulations of integers are efficiently implemented in most programming languages [18].

As the dimensionality of the Hilbert space in this basis grows exponentially ($d_{HB} = 2^L$), the generated matrix can be considered to be very large even for moderate sized systems[1]. Fortunately, it can also be considered to be sparse, as there are only on the order of L non-zero elements in each column. Thus, it is necessary to implement a scheme as *Lanczos diagonalization* to solve the final eigenvalue problem. To further improve performance and expand the limit of solvable systems, one may exploit symmetries of both the Hamiltonian itself and the lattice to block diagonalize the matrix [5, pp 352-354]. For example, using the rotation symmetry of the Hamiltonian, implying that total spin along the z-axis

$$S^z = \sum_i s_i$$

is preserved, subspaces of specific S^z can be diagonalized separately, reducing the computational effort significantly.

B.2 Hubbard model

In the spin-charge separated basis for the half-filled Hubbard model, presented in section 4.1, an approach of labeling the basis states can be found as an extension of the binary-spin array above. One may simply use two binary

[1] Here, matrices exceeding 10000×10000 can be considered *very large* [5, p 343], corresponding to roughly 13 half-spins.

strings, and let the quasi-spin and quasi-charge states be encoded into separate binary strings. The labeling definition can then be written:

$$\tilde{I}_\phi = \sum_{i=1}^{L} \left(b_i 2^{i-1} + b'_i 2^{L+i-1} \right) , \quad b_i = \frac{1}{2} + q_i^z , \quad b'_i = \tilde{n}_i .$$

Disregarding the unphysical states with odd charge number, the dimensionality of the Hilbert space is $d_H = 2^{(2L-1)}$ for a L-spin system in this basis.

The evaluation of the matrix elements is slightly more complicated, as one must also consider possible phase factors from the fermionic charge operators in the Hamiltonian:

$$\tilde{\mathscr{H}} = t \left(T_0 + T_\pm \right) + U h_u ,$$

with

$$\begin{aligned} T_\pm &= 2 \sum_i (-1)^i \left(\frac{1}{4} - \boldsymbol{q}_i \cdot \boldsymbol{q}_{i+1} \right) \left(\tilde{c}_i^\dagger \tilde{c}_{i+1}^\dagger + \tilde{c}_{i+1} \tilde{c}_i \right) &&\equiv \sum_i T_{i,i+1}^{(\pm)} , \\ T_0 &= 2 \sum_i \left(\frac{1}{4} + \boldsymbol{q}_i \cdot \boldsymbol{q}_{i+1} \right) \left(\tilde{c}_i^\dagger \tilde{c}_{i+1} + \tilde{c}_{i+1}^\dagger \tilde{c}_i \right) &&\equiv \sum_i T_{i,i+1}^{(0)} , \\ h_U &= \frac{1}{2} \sum_i \tilde{c}_i^\dagger \tilde{c}_i , \end{aligned}$$

where $i+1 = L+1$ is taken to be equal to one, and $(-1)^i = \pm 1$ for i even and odd, respectively. Treatment of the diagonal interaction term h_u is trivial, and also the quasi-spin factor of the kinetic terms is straight forward, following the treatment for the Heisenberg model.

The $T_\pm$ term

Fixing the phase of a basis state with some charge configuration by defining it as a sequence of charge operators operating onto a uncharged spin state:

$$|\phi\rangle \equiv \tilde{c}_{k_1}^\dagger \tilde{c}_{k_2}^\dagger \ldots \tilde{c}_{k_n}^\dagger \, |q_1, q_2, \ldots q_L\rangle , \quad 1 \le k_1 < k_2 < \ldots < k_n \le L ,$$

Then, first consider the action of $\tilde{c}_i^\dagger \tilde{c}_{i+1}^\dagger$ for $1 \le i \le L-1$ onto this state[2]:

$$\tilde{c}_i^\dagger \tilde{c}_{i+1}^\dagger \, |\phi\rangle = \tilde{c}_i^\dagger \tilde{c}_{i+1}^\dagger \left(\tilde{c}_{k_1}^\dagger \ldots \tilde{c}_{k_l}^\dagger \tilde{c}_{k_m}^\dagger \ldots \tilde{c}_{k_n}^\dagger \right) |q_1 \ldots q_L\rangle , \quad k_l < i , i+1 < k_m ,$$

and one finds the result after commutating the operators to the correct position in the sequence:

$$\tilde{c}_i^\dagger \tilde{c}_{i+1}^\dagger \, |\phi\rangle = (-1)^{2l} \Big(\underbrace{\tilde{c}_{k_1}^\dagger \ldots \tilde{c}_{k_l}^\dagger}_{l \text{ ops.}} \tilde{c}_i^\dagger \tilde{c}_{i+1}^\dagger \tilde{c}_{k_m}^\dagger \ldots \tilde{c}_{k_n}^\dagger \Big) \, |q_1 \ldots q_L\rangle ,$$

[2] In the following, it is assumed that the states considered are such that none of the the charge operators applied trivially annihilate the state.

where l is the number of operators in the sequence for which $k_r < i$. Similarly, for the annihilation term one obtains:

$$\begin{aligned}\tilde{c}_{i+1}\tilde{c}_i\,|\phi'\rangle &= \tilde{c}_{i+1}\tilde{c}_i\left(\tilde{c}^\dagger_{k_1}\ldots\tilde{c}^\dagger_{k_l}\tilde{c}^\dagger_i\tilde{c}^\dagger_{i+1}\tilde{c}^\dagger_{k_m}\ldots\tilde{c}^\dagger_{k_n}\right)|q_1\ldots q_L\rangle \\ &= (-1)^{2l}\Big(\underbrace{\tilde{c}^\dagger_{k_1}\ldots\tilde{c}^\dagger_{k_l}}_{l\text{ ops.}}\tilde{c}^\dagger_{k_m}\ldots\tilde{c}^\dagger_{k_n}\Big)|q_1\ldots q_L\rangle\ .\end{aligned}$$

The term operating over the periodic boundary is particular:

$$\tilde{c}^\dagger_L\tilde{c}^\dagger_1\,|\phi\rangle = \tilde{c}^\dagger_L\tilde{c}^\dagger_1\Big(\tilde{c}^\dagger_{k_1}\ldots\tilde{c}^\dagger_{k_n}\Big)|q_1\ldots q_L\rangle = (-1)^{n+1}\Big(\tilde{c}^\dagger_1\underbrace{\tilde{c}^\dagger_{k_1}\ldots\tilde{c}^\dagger_{k_n}}_{n\text{ ops.}}\tilde{c}^\dagger_L\Big)|q_1\ldots q_L\rangle\ ,$$

and

$$\begin{aligned}\tilde{c}_1\tilde{c}_L\,|\phi'\rangle &= \tilde{c}_1\tilde{c}_L\Big(\tilde{c}^\dagger_1\tilde{c}^\dagger_{k_2}\ldots\tilde{c}^\dagger_{k_{n-1}}\tilde{c}^\dagger_L\Big)|q_1\ldots q_L\rangle \\ &= (-1)^{n-1}\Big(\underbrace{\tilde{c}^\dagger_{k_2}\ldots\tilde{c}^\dagger_{k_{n-1}}}_{n-2\text{ ops.}}\Big)|q_1\ldots q_L\rangle\ .\end{aligned}$$

As $2l$ is even and $n\pm1$ is odd, as n must be even for physical states, the matrix element for the boundary term in $T_\pm$ picks up an extra sign.

The T_0 term

Continuing the calculation as above one finds for $1 \le i \le L-1$:

$$\tilde{c}^\dagger_i\tilde{c}_{i+1}\,|\phi\rangle = \tilde{c}^\dagger_i\tilde{c}_{i+1}\left(\tilde{c}^\dagger_{k_1}\ldots\tilde{c}^\dagger_{k_l}\tilde{c}^\dagger_{i+1}\tilde{c}^\dagger_{k_m}\ldots\tilde{c}^\dagger_{k_n}\right)|q_1\ldots q_L\rangle\ ,\quad k_l < i\,, i{+}1 < k_m\,,$$

so that

$$\tilde{c}^\dagger_i\tilde{c}_{i+1}\,|\phi\rangle = \tilde{c}^\dagger_i\tilde{c}_{i+1} = (-1)^{2l}\Big(\underbrace{\tilde{c}^\dagger_{k_1}\ldots\tilde{c}^\dagger_{k_l}}_{l\text{ ops.}}\tilde{c}^\dagger_i\tilde{c}^\dagger_{k_m}\ldots\tilde{c}^\dagger_{k_n}\Big)|q_1\ldots q_L\rangle\ ,$$

and also the term for $\tilde{c}^\dagger_{i+1}\tilde{c}_i$ has an even number of sign factors.

Finally, fermionic sign factor the periodic terms are calculated to be:

$$\tilde{c}^\dagger_L\tilde{c}_1\,|\phi\rangle = \tilde{c}^\dagger_L\tilde{c}_1\left(\tilde{c}^\dagger_1\tilde{c}^\dagger_{k_2}\ldots\tilde{c}^\dagger_n\right)|q_1\ldots q_L\rangle = (-1)^{n-1}\Big(\underbrace{\tilde{c}^\dagger_{k_2}\ldots\tilde{c}^\dagger_{k_n}}_{n-1\text{ ops.}}\tilde{c}^\dagger_L\Big)|q_1\ldots q_L\rangle\ .$$

Again, the $\tilde{c}^\dagger_1\tilde{c}_L$ term is treated similarly and one finds that also the matrix element for the periodic term in T_0 has an extra sign factor.

Appendix C

The Valence bond basis and Singlet projection operators

Here follows a short summary of the construction and properties of the valence bond basis as presented by Beach and Sandvik [10].

When working with the singlet sector of the Hubbard model it may be convenient use the *valence bond* basis instead of using the "traditional" basis of S^z eigenstates. In the valence bond basis, states are represented by a particular way of pairing up the spins into singlets

$$|\psi\rangle = \prod_p (i_p, j_p) \ , \quad (i,j) = \frac{1}{\sqrt{2}}\Big(|\uparrow_i\downarrow_j\rangle - |\downarrow_i\uparrow_j\rangle \Big),$$

and from this construction the valence bond states are invariant under spin rotations.

C.1 Valence bond operators

The spin operators are written using bosonic operators $b_{i,s}$ and a occupation constraint of one bosonic particle per site:

$$\boldsymbol{S}_i = \frac{1}{2}\sum_{s,s'} b^\dagger_{i,s}\boldsymbol{\sigma}_{s,s'}b_{i,s'} \ , \quad \sum_s b^\dagger_{i,s}b_{i,s} = 1 \, ,$$

and the *valence bond operator* is defined by:

$$\chi^{\mu\dagger}_{ij} = \frac{1}{\sqrt{2}}\sum_{s,s'} \tau^\mu_{s,s'} b^\dagger_{i,s} b^\dagger_{j,s'} \ , \quad \tau^\mu = (i\sigma^2,\, i\sigma^3,\, 1\,, -i\sigma^1) \, .$$

These valence bond operators create eigenstates of the singlet projection operator $Q_{ij} = 1/4 - \boldsymbol{S}_i \cdot \boldsymbol{S}_j$, corresponding to one singlet ($\mu = 0$) and three

triplets:

$$\chi_{ij}^{\mu\dagger}\left|vac\right\rangle = \begin{cases} \frac{1}{\sqrt{2}}\left(\left|\uparrow_i\downarrow_j\right\rangle - \left|\downarrow_i\uparrow_j\right\rangle\right), & \mu = 0\,, \\ \frac{1}{\sqrt{2}}\left(\left|\uparrow_i\uparrow_j\right\rangle - \left|\downarrow_i\downarrow_j\right\rangle\right), & \mu = 1\,, \\ \frac{1}{\sqrt{2}}\left(\left|\uparrow_i\uparrow_j\right\rangle + \left|\downarrow_i\downarrow_j\right\rangle\right), & \mu = 2\,, \\ \frac{1}{\sqrt{2}}\left(\left|\uparrow_i\downarrow_j\right\rangle + \left|\downarrow_i\uparrow_j\right\rangle\right), & \mu = 3\,, \end{cases}$$

so that:

$$Q_{ij}\chi_{ij}^{\mu\dagger}\left|vac\right\rangle = \delta^{\mu 0}\chi_{ij}^{\mu\dagger}\left|vac\right\rangle\,.$$

Using the completeness relation:

$$\sum_{\mu}\chi_{ij}^{\mu\dagger}\chi_{ij}^{\mu} = 1\,,$$

and

$$\boldsymbol{S}_i\cdot\boldsymbol{S}_j = -\frac{3}{4}\chi_{ij}^{0\dagger}\chi_{ij}^{0} + \frac{1}{4}\boldsymbol{\chi}_{ij}^{\dagger}\cdot\boldsymbol{\chi}_{ij}\,.$$

which follows from construction, one may write the singlet projection operator using valence bond operators:

$$Q_{ij} = \chi_{ij}^{0\dagger}\chi_{ij}^{0}\,.$$

C.2 AB-Valence bond basis

The basis states of the *valence bond basis* are formed by creating singlets out of pairs of spins in a lattice of size N, using the singlet valence bond operator defined above. A valence bond state $\left|V\right\rangle$ is then written:

$$\left|V\right\rangle = V^{\dagger}\left|vac\right\rangle = \prod_{b}\chi_{i_b j_b}^{0\dagger}\left|vac\right\rangle\,,$$

and the basis defined by this spans the $S = 0$ subspace for a system consisting of an even number of spin-half particles.

Dividing the square lattice into two disjoint sublattices A and B containing $N/2$ sites each, the basis can be restricted to singlets only connecting spins on different sublattices. The number of states in this AB-restricted valence bond basis is reduced from $N!$ to $(N/2)!$, but it still spans the singlet sector, as any AA or BB-bond can be rewritten using only AB-bonds from the relation:

$$\chi_{ij}^{0\dagger}\chi_{kl}^{0\dagger} + \chi_{il}^{0\dagger}\chi_{jk}^{0\dagger} + \chi_{lj}^{0\dagger}\chi_{ik}^{0\dagger} = 0\,.$$

The restriction to AB-singlet bonds also gives a way of specifying a sign convention for the valence bond states, relating to the corresponding valence bond operator, so that $\chi_{ij}^{0\dagger} = -\chi_{ji}^{0\dagger}$ creates a singlet with $i \in A$ and $j \in B$.

C.3 Singlet projection in the valence bond basis

Under repeated applications of singlet projection operators Q_{ij}, as when projecting out the ground state, the valence bond states evolves by remapping the singlet pairing in the states.

Starting with the action of Q_{ij} onto valence bond state $|V\rangle$:

$$Q_{ij}\,|V\rangle = \chi^{0\dagger}_{ij}\chi^{0}_{ij}\,V^{\dagger}\,|vac\rangle = \chi^{0\dagger}_{ij}\chi^{0}_{ij}\left(\chi^{0\dagger}_{a_1b_1}\chi^{0\dagger}_{a_2b_2}\cdots\chi^{0\dagger}_{a_Nb_N}\right)|vac\rangle\ ,$$

and assuming that the string $V^{\dagger}$ contains a valence bond operator matching the indices of the singlet projection operator Q_{ij}, i.e. $(a_m, b_m) = (i, j)$. Then, through the use of

$$[\chi^{0}_{ij}, \chi^{0\dagger}_{ij}]\,|vac\rangle = |vac\rangle\ ,$$

one finds

$$\begin{aligned} Q_{ij}\,|V\rangle &= \chi^{0\dagger}_{ij}\left[\chi^{0}_{ij}, \left(\chi^{0\dagger}_{a_1b_1}\chi^{0\dagger}_{a_2b_2}\cdots\chi^{0\dagger}_{ij}\cdots\chi^{0\dagger}_{a_Nb_N}\right)\right]|vac\rangle \\ &= \chi^{0\dagger}_{ij}\left(\chi^{0\dagger}_{a_1b_1}\chi^{0\dagger}_{a_2b_2}\cdots\chi^{0\dagger}_{a_Nb_N}\right)|vac\rangle = |V\rangle\ . \end{aligned}$$

Thus, this state is an eigenstate of Q_{ij} with eigenvalue 1.

If there is no matching valence bond operator in $V^{\dagger}$, then there must be two operators $\chi^{0\dagger}_{il}$ and $\chi^{0\dagger}_{kj}$ in $V^{\dagger}$, each matching one of the indices in Q_{ij}. Now, using the relation:

$$[\chi^{0}_{ij}, \chi^{0\dagger}_{il}\chi^{0\dagger}_{kj}]\,|vac\rangle = \frac{1}{2}\chi^{0\dagger}_{kl}\,|vac\rangle\ ,$$

the action of the singlet projection operator is found to be

$$\begin{aligned} Q_{ij}\,|V\rangle &= \chi^{0\dagger}_{ij}\left[\chi^{0}_{ij}, \left(\chi^{0\dagger}_{a_1b_1}\chi^{0\dagger}_{a_2b_2}\cdots\chi^{0\dagger}_{il}\cdots\chi^{0\dagger}_{kj}\cdots\chi^{0\dagger}_{a_Nb_N}\right)\right]|vac\rangle \\ &= \frac{1}{2}\chi^{0\dagger}_{ij}\left(\chi^{0\dagger}_{a_1b_1}\chi^{0\dagger}_{a_2b_2}\cdots\chi^{0\dagger}_{kl}\cdots\chi^{0\dagger}_{a_Nb_N}\right)|vac\rangle = \frac{1}{2}\,|V'\rangle\ . \end{aligned}$$

Here the singlet projection operator modifies the initial valence bond state so that two of the singlets in $|V\rangle$ are reconfigured, giving a modified state $|V'\rangle$ and also adds a factor $1/2$ to the amplitude of the state.

Appendix D

Monte Carlo Simulations using the Metropolis algorithm

Monte Carlo methods allow for making effective approximative evaluations of various expectance values from a broad class of problems in statistical and quantum physics [11, pp 185]. In classical statistical physics, a general expectance value of some quantity is expressed as a weighted sum of the state-specific value of the quantity over the available states in the phase space of the system

$$\langle \mathscr{A} \rangle = \frac{1}{Z} \sum_{S \in \Omega} W(S) \mathscr{A}(S) \,, \quad Z = \sum_{S \in \Omega} W(S) \,.$$

D.1 The Metropolis algorithm

An approximate value for this expression can now be obtained by the Metropolis algorithm, in which a *Markov chain* of states $S^{(1)}, S^{(2)}, \ldots$ distributed with probability density $W(S)/Z$, is formed by a random walk through phase space. The expenction value is then computed by sampling the quantity in question for the states visited

$$\langle \mathscr{A} \rangle = \frac{1}{N} \sum_{n=1}^{N} \mathscr{A}(S^{(n)}) \,, \quad N \to \infty \,.$$

For the states found in the Markov chain to be of the desired distribution, it is sufficient to construct an *ergodic* random walk in which the probability of making a step from S to S' satisfies *detailed balance* [15]. Finite ergodic Markov chains have a well defined limit distribution, independently of starting position [19] and the condition of detailed balance assures that this limit distribution is proportional to the statistical weights of the physical system. For finite Markov chains, irreducibility and non-periodicity implies ergodicity.

In the Metropolis algorithm the state $S' = S^{(n+1)}$ in the sequence is generated from the $S = S^{(n)}$ in an updating scheme performed in two distinct steps, where the first consisting of generating a suggested update, or a *trial state*, and then accepting or rejecting that update. The total transition probability $p(S \to S')$ of the update is then also split into two factors corresponding to the probabilities of the two distinct steps of the transition $S \to S'$

$$p(S \to S') = t(S \to S')a(S \to S')\,,$$

where $t(S \to S')$ and $a(S \to S')$ denote the probabilities of choosing the specific trial step by the updating algorithm used and accepting it, respectively.

The condition of detailed balance [15]:

$$W(S)p(S \to S') = W(S')p(S' \to S)$$

is satisfied if the trial states are generated such

$$t(S \to S') = t(S' \to S)\,,$$

and the acceptance probability of the generated trial states is set as

$$a(S \to S') = min\left(\frac{W(S')}{W(S)}, 1\right)\,.$$

D.2 Autocorrelation and error estimation

The major drawback of using an random walk to generate states of a specific distribution, as in the Metropolis algorithm, is that the sequence of states are not independent of one another. It is then necessary to consider these correlations to ensure convergence of the simulation and to make accurate error calculations [15].

The *autocorrelation function* for samples of a quantity $\mathscr{A}$ from the sequence of configurations in the Markov chain is defined as [5, p 193]:

$$C(k) = \langle \mathscr{A}_n \mathscr{A}_{n+k} \rangle - \langle \mathscr{A}_n \rangle^2\,.$$

From this, the normalized *integrated correlation time* is formed:

$$\tau = \sum_{k=-K}^{K} \frac{C(k)}{C(0)}\,, \quad K \to \infty\,.$$

Finally, the estimation of the statistical error in the calculated quantity is found by considering the statistical error estimate assuming uncorrelated samples, and then introducing a correction to the number of actual (uncorrelated) samples used:

$$\epsilon = \frac{\sigma(\mathscr{A}_n)}{\sqrt{N/\tau}}\,.$$

Bibliography

[1] P. Fazekas, *Lecture Notes on Electron Correlation and Magnetism*. World Scientific Publishing Co. Pte. Ltd., 1999.

[2] P. W. Anderson, "Personal history of my engagement with cuprate superconductivity, 1986-2010," *arXiv:1011.2736v1 [cond-mat.supr-con]*, 2010.

[3] F. Anfuso, *Strongly Interacting Electrons in One and Two Dimensions*. PhD thesis, Chalmers University of Technology, 2006.

[4] H. Sandström, "Spin-charge separation in the Hubbard model," Master's thesis, Göteborg University, 2007.

[5] J. M. Thijssen, *Computational Physics*. Cambridge University Press, 2007.

[6] A. W. Sandvik, "Finite-size scaling of the ground-state parameters of the two-dimensional Heisenberg model," *Phys. Rev. B*, vol. 56, no. 18, pp. 11678–11690, 1997.

[7] A. W. Sandvik, "Ground state projection of quantum spin systems in the valence-bond basis," *Phys. Rev. Lett.*, vol. 95, no. 20, p. 207203, 2005.

[8] A. W. Sandvik and K. S. D. Beach, "Monte carlo simulations of quantum spin systems in the valence bond basis," *arXiv:0704.1469v1 [cond-mat.str-el]*, 2007.

[9] E. H. Lieb, "Two theorems on the Hubbard model," *Physical Review Letters*, vol. 62, no. 10, pp. 1201–1204, 1989.

[10] K. Beach and A. W. Sandvik, "Some formal results for the valence bond basis," *Nuclear Physics B*, vol. 750, pp. 142–178, 2006.

[11] S. E. Koonin, *Computational Physics*. The Benjamin/Cummings Publishing Company, Inc., 1986.

[12] V. Ambegaokar and M. Troyer, "Estimating errors reliably in monte carlo simulations of the ehrenfest model," *American Journal of Physics*, vol. 78, no. 2, pp. 150–157, 2010.

[13] S. Östlund and M. Granath, "Exact transformation for spin-charge separation of spin-1/2 fermions without constraints," *Physical Review*, vol. 96, no. 6, p. 066404, 2006.

[14] A. W. Sandvik and H. G. Evertz, "Loop updates for variational and projector quantum monte carlo simulations in the valence-bond basis," *Phys. Rev. B*, vol. 82, no. 2, p. 024407, 2010.

[15] H. Evertz, "The loop algorithm," *Advances in Physics*, vol. 52, no. 1, pp. 1–66, 2003.

[16] C. Kittel, *Introduction to Solid State Physics*, pp. 232–235. John Wiley & Sons, Inc, 2005.

[17] E. H. Lieb and F. Y. Wu, "The one-dimensional Hubbard model: a reminiscence," *Physica A: Statistical Mechanics and its Applications*, vol. 321, no. 1-2, pp. 1–27, 2003.

[18] S. A. Jafari, "Introduction to Hubbard model and exact diagonalization," *Iranian Journal of Physics Research*, vol. 8, 2008.

[19] J. Enger and J. Grandell, *Markovprocesser och köteori*, p. 34. Matematisk Statistik, Chalmers & GU.